

AD-A084 906

NAVAL SURFACE WEAPONS CENTER SILVER SPRING MD  
F/6 21/9-2  
DOT BEHAVIOR OF POROUS PROPELLANT MODELS AND POROUS SAMPLES OF --ETC(U)  
MAR 80 D PRICE, R R BERNECKER

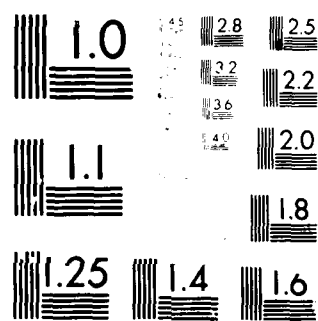
UNCLASSIFIED

NSWC/TR-80-65

NL

1 OF 1  
AD-A084 906

END  
DATE FILMED  
6-80  
DTIC



MICROCOPY RESOLUTION TEST CHART  
NATIONAL BUREAU OF STANDARDS-1963-3

DDC FILE COPY.

ADA 084906

b2  
NSWC TR 80-65

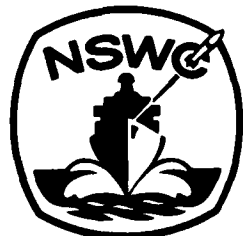
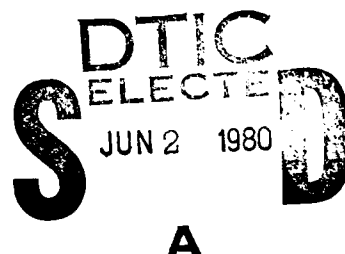
LEVEL II  
2

## DDT BEHAVIOR OF POROUS PROPELLANT MODELS AND POROUS SAMPLES OF COMMERCIAL PROPELLANTS

BY DONNA PRICE RICHARD R. BERNECKER  
RESEARCH AND TECHNOLOGY DEPARTMENT

13 MARCH 1980

Approved for public release, distribution unlimited.



### NAVAL SURFACE WEAPONS CENTER

Dahlgren, Virginia 22448 • Silver Spring, Maryland 20910

80 5 30 033

## UNCLASSIFIED

SECURITY CLASSIFICATION OF THIS PAGE (When Data Entered)

REPORT DOCUMENTATION PAGE		READ INSTRUCTIONS BEFORE COMPLETING FORM
1. REPORT NUMBER 14 NSWC/TR-80-65	2. GOVT ACCESSION NO.	3. RECIPIENT'S CATALOG NUMBER
4. TITLE (including subtitle) DDI BEHAVIOR OF POROUS PROPELLANT MODELS AND POROUS SAMPLES OF COMMERCIAL PROPELLANTS		5. TYPE OF REPORT & PERIOD COVERED
6. AUTHOR(s) 10 Donna Price and Richard R. Bernecker		6. PERFORMING ORG. REPORT NUMBER
7. PERFORMING ORGANIZATION NAME AND ADDRESS Naval Surface Weapons Center White Oak Silver Spring, Maryland 20910		8. CONTRACT OR GRANT NUMBER(s) 16
9. CONTROLLING OFFICE NAME AND ADDRESS		10. PROGRAM ELEMENT, PROJECT, TASK AREA & WORK UNIT NUMBERS 61152N, ZR00001 ZR01305
11. MONITORING AGENCY NAME & ADDRESS (if different from Controlling Office)		12. REPORT DATE 13 March 1980
14. DISTRIBUTION STATEMENT (of this Report) Approved for public release, distribution unlimited.		14 12 44 15. SECURITY CLASS. (of this report) Unclassified
16. DISTRIBUTION STATEMENT (of the abstract entered in Block 20, if different from Report) 17 ZR01305 ZR01309		15a. DECLASSIFICATION/DOWNGRADING SCHEDULE
18. SUPPLEMENTARY NOTES		
19. KEY WORDS (Continue on reverse side if necessary and identify by block number) DDT Detonation Sensitivity Explosives      Propellants Combustion Flame spreading		
20. ABSTRACT (Continue on reverse side if necessary and identify by block number) A number of binary mixtures, components of which are propellant ingredients, were examined in steel walled tubes for their DDT behavior at 60-70% theoretical maximum density (TMD). Several commercial propellants and one 4-component, composite model were also examined. A number of compositional effects were noted and reported. Some propellants, at high porosity, showed reaction not detectable by our ionization probes. For propellants which exhibited transition at 70% TMD in our apparatus, the range in predetonation		

**UNCLASSIFIED**

SECURITY CLASSIFICATION OF THIS PAGE (When Data Entered)

20. (Cont.)

column length ( $l$ ) was 103-170 mm and in relative time to detonation, 76-247  $\mu$ s.

M.C.A.

**UNCLASSIFIED**

SECURITY CLASSIFICATION OF THIS PAGE (When Data Entered)

FOREWORD

This report was prepared under Task ZR0130901, IR-159. The work was an exploratory investigation to obtain an overview of propellant sensitivity to deflagration to detonation transition (DDT). The present results and conclusions on the DDT behavior of highly porous propellant models and propellants should be of interest in the areas of explosive sensitivity and of propellant safety.

*John M Blatstein for*  
JULIUS W. ENIG  
By direction

Accession For	
NTIS	Classified
DDC TAB	<input checked="" type="checkbox"/>
Unclassified	<input type="checkbox"/>
Information	<input type="checkbox"/>
By _____	
Distribution	
Availability	
Dist	Available or Special

*A*

## CONTENTS

	<u>Page</u>
INTRODUCTION . . . . .	1
EXPERIMENTAL . . . . .	1
Instrumentation and Procedures . . . . .	1
Materials . . . . .	2
EXPERIMENTAL RESULTS AND DISCUSSION . . . . .	3
SUMMARY AND CONCLUSIONS . . . . .	7
BIBLIOGRAPHY . . . . .	8
APPENDIX A - DETAILED DISCUSSION OF RECORDED DATA . . . . .	A-1

## ILLUSTRATIONS

<u>Figure</u>		<u>Page</u>
A1	DISTANCE-TIME DATA FROM SHOT 805 ON 80/20 AP/WAX AT 67.0% TMD, $\rho_0 = 1.10 \text{ g/cm}^3$	A-11
A2	DISTANCE-TIME DATA FROM SHOT 809 ON 80/20 AP/WAX AT 56.6% TMD, $\rho_0 = 0.93 \text{ g/cm}^3$	A-11
A3	DISTANCE-TIME DATA FROM SHOT 906 ON 80/20 AP/Al AT 56.8% TMD, $\rho_0 = 1.17 \text{ g/cm}^3$	A-12
A4	DISTANCE-TIME DATA FROM SHOT 1012 ON 91/9 RDX/Al AT 89.6% TMD, $\rho_0 = 1.67 \text{ g/cm}^3$	A-12
A5	DATA FROM SHOT 1109 ON 91/9 RDX/WAX AT 71.2% TMD, $\rho_0 = 1.32 \text{ g/cm}^3$	A-13
A6	DATA FROM SHOT 1118 ON 80/20 RDX/WAX AT 89.8% TMD, $\rho_0 = 1.73 \text{ g/cm}^3$	A-14
A7	DATA FROM SHOT 1203 on 80/20 RDX/Al at 70.4% TMD, $\rho_0 = 1.36 \text{ g/cm}^3$	A-15
A8	DATA FROM SHOT 810 ON NC AT 59.9% TMD, $\rho_0 = 0.95 \text{ g/cm}^3$	A-16

## NSWC TR 80-65

## ILLUSTRATIONS (Cont.)

<u>Figure</u>		<u>Page</u>
A9	DATA FROM SHOT 905 ON 80/20 NC/A <sub>2</sub> AT 57.0% TMD, $\rho_0 = 0.98 \text{ g/cm}^3$ . . . . .	A-17
A10	DATA FROM SHOT 1101 ON NC AT 69.4% TMD, $\rho_0 = 1.10 \text{ g/cm}^3$ . . . . .	A-18
A11	DISTANCE-TIME DATA FROM SHOT 1008 ON 85/15 NC/AP AT 69.8% TMD, $\rho_0 = 1.14 \text{ g/cm}^3$ . . . . .	A-19
A12	DISTANCE-TIME DATA FROM SHOT 1005 ON 91/9 HMX/AP AT 69.5% TMD, $\rho_0 = 1.32 \text{ g/cm}^3$ . . . . .	A-19
A13	DATA FROM SHOT 707 ON 57.3% TMD 25/5/20/50 NC/AP/A <sub>2</sub> /HMX, $\rho_0 = 1.11 \text{ g/cm}^3$ . . . . .	A-20
A14	DATA FROM SHOT 816 ON 67.5% TMD DOUBLE BASE POWDER M-7, $\rho_0 = 1.10 \text{ g/cm}^3$ . . . . .	A-21

## TABLES

<u>Table</u>		<u>Page</u>
1	SUMMARY OF RESULTS . . . . .	4
A1	MEASURED AND ASSIGNED $\rho$ VALUES . . . . .	A-6
A2	DETAILED DATA FOR DDT EXPERIMENTS WITH VARIOUS MATERIALS . . . . .	A-7

## INTRODUCTION

The present work was undertaken as an exploratory investigation of propellant (i.e., composite explosive) sensitivity to undergoing a transition from burning to detonation. The tendency of a propellant to exhibit a deflagration to detonation transition (DDT) is becoming increasingly important as propellant grains are made larger and the amount of their explosive component (e.g. HMX, NC, NG) is increased. It was the purpose of this preliminary work to obtain a broad overview, with large variations in composition, of this sensitivity area in order to select a good experimental approach for its study.

It is generally recognized that the explosive behavior of propellants is greatly enhanced by the presence of porosity. Hence the experimental work was carried out at about 60-70% theoretical maximum density (TMD). A systematic variation of the porosity or of the compositions was not attempted at this time.

The charges used consisted of a single propellant component which is also a high explosive, nitrocellulose (NC), various mechanical binary mixtures consisting of pairs to be found in commercial propellants and composite explosives, and a single 4-component model. The commercial propellants examined were a gun propellant (M-7, essentially a double base NC/NG composition), a gas generator (Arcadene, plastic bonded HMX), and two rocket propellants (FKM and VLU). FKM is a composite propellant with HMX added; VLU is a composite modified double base (CMDB) propellant and is also referred to as a cross-linked double base (XLDB) propellant.

## EXPERIMENTAL

INSTRUMENTATION AND PROCEDURES

The experimental setup and procedures have been described in detail elsewhere<sup>1,2</sup>. The apparatus consists of a seamless steel tube with heavy end closures. The column length of the 0.35 g of 25/75 B/KNO<sub>3</sub> ignitor is 6.3 mm; the length of the explosive column is 295.4 mm. Each pressed charge is examined by X-ray prior to its instrumentation.

<sup>1</sup>Bernecker, R. R. and Price, D., "Studies in the Transition from Deflagration to Detonation in Granular Explosives," Combust. Flame, Vol. 22, 1974, 111-117, 119-129, and 161-170. See also NOLTR 72-202.

<sup>2</sup>Price, D. and Bernecker, R. R., "Sensitivity of Porous Explosives to Transition from Deflagration to Detonation," Combust. Flame, Vol. 25, 1975, 91-100. See also NOLTR 74-186.

The DDT tube is instrumented with ionization probes (IP) and strain gages (SG) to monitor ionization fronts and internal pressure, respectively. For brevity, henceforth ionization probes will be referred to as probes; strain gages, as gages. As before<sup>1</sup>, both custom-made and commercial probes are used; distance-time (x-t) data from each are distinguished on the graphs. The number of gage locations for monitoring internal pressure is generally four or five per tube. The gage output is reported in strain ( $\epsilon$ ) or microstrain ( $\mu\epsilon$ ). In a static calibration of the tube, the gradient is  $112 \mu\epsilon/\text{kbar}$  up to the elastic limit at 2.2 kbar. From 2 to 4.7 kbar, the microstrain increases from 225 to 788.

One difference in procedure from that reported in Reference 1 is in the determination of the predetonation column length,  $\ell$ . In the case of 91/9 RDX/wax, it was possible to use the intersection of the postconvective wave front with the extrapolated detonation front to locate  $\ell$  in the x-t plane; the value was confirmed by that obtained from tube fragments. Here and, in general for HE other than 91/9 RDX/wax,  $\ell$  is more reliably determined from markings on the tube fragments; it is checked for consistency with the probe and gage records in the x-t plane. In the present work, there were a few shots for which tube fragments did not give an unambiguous value of  $\ell$ . These are discussed in the Appendix and listed in Table A1. Unless otherwise indicated,  $\ell$  values were measured to  $\pm 3 \text{ mm}$ .

Values for x were measured from the ignitor/explosive interface. Relative time values were measured from the first discharge of the triggering IP; this was generally the first probe.

#### MATERIALS

The ammonium perchlorate (AP) used was propellant grade and contained 0.2% tricalcium phosphate. It was ground at the Naval Ordnance Station (Indian Head, MD). The lot used for this work had a weight mean particle size of  $8 \mu\text{m}$  by micromerograph. The aluminum used was dichromated spherical powder supplied by Valley Metallurgical Processing Company. It was designated H-5 and had an average particle size of  $7 \mu\text{m}$  by Fisher subsieve sizer. The wax used was a refined, powdered, grade 1 yellow carnauba wax supplied by Frank B. Ross Company; its average particle size was about  $125 \mu\text{m}$ . The explosives were obtained commercially and satisfied the relevant military specifications. RDX was Class A ( $\delta \sim 200\mu$ ); HMX, Class E ( $\delta \sim 15\mu$ ). The nitrocellulose (NC) was obtained through NOS, Indian Head, MD. It was an Olin Matheson fluid ball powder, Type A; it is essentially NC ( $\delta \sim 40\mu$ ) which is nominally 12.6% nitrogen and contains about 1% 2-nitrodiphenylamine stabilizer and 0.2-0.3% coating material. The gun propellant, a modified M-7, was also obtained from NOS/IH, and shredded in our Laboratory (See Appendix). The other three propellants, in shredded or powdered form, were obtained from their respective manufacturers. All dry mixing was carried out by the procedure of Reference 3.

<sup>3</sup>Price, D., Clairmont, A. R., Jr., and Erkman, J. O., "Explosive Behavior of Aluminized Ammonium Perchlorate," Combust. Flame, Vol. 20, 1973, 389-400.

## EXPERIMENTAL RESULTS AND DISCUSSION

A total of fifteen shots were made. Detailed tables, records for each shot, and discussions of them appear in the Appendix. Table 1 contains a summary of the results. As that tabulation shows, the charges have been divided into four groups; that classification is roughly in accord with their composition.

The first group consisted of binary AP mixtures that might be expected in composite or CMDB propellants. Each of the three charges was 80% AP. AP/wax was fired at 56.6 and 67.0% TMD; AP/Al, at 56.8% TMD. As Table 1 shows, all three failed to transit to detonation, but all three burned readily. In fact, the velocities of the reactive fronts detected by IPs are much higher than would be expected for a convective front at these high porosities. Russian workers<sup>4</sup> report that the breakdown of conductive burning and the appearance of convective burning occurs for AP/bitumen mixtures at a much lower critical pressure than it does for organic HE. This is probably also the case for AP/wax, and, if so, the burning is already greatly accelerated by the time of response of the IP 41 mm from the igniter. The same effect was seen in AP/Al where the first IP was at  $x = 80$  mm. In every case, the velocity of the IP front was no longer accelerating; it was either constant or falling slightly. Other Russian workers<sup>5</sup> have reported that a stoichiometric mixture of AP/polystyrene did exhibit DDT at 40 and 55% TMD, but not at 75% TMD. Thus it is possible that the three AP mixes at larger porosities or different compositions or both would show a transition. All three are detonable under shock initiation.

The second charge group consisted of binary mixes of RDX/Al which might appear in either a CMDB or a composite propellant to which RDX has been added. The Al content was 9 or 20% and each composition was tested at 70 and 90% TMD; all exhibited DDT. Again, as in the previous group, by the time the reaction had reached the first IP, it was well advanced in the two charges with 9% Al. RDX (10-20 $\mu$ ) has a critical breakdown pressure about twice that of the AP mixture<sup>4</sup> but the RDX used here with  $\delta \sim 200\mu$  will have a lower breakdown pressure. Moreover, its acceleration after the onset of the convective flame front may be greater. When the Al content was increased to 20%, the transition was sufficiently slowed to exhibit an IP front velocity of the magnitude of that expected for a convective flame front at the given porosity. Increasing the porosity also slowed down the DDT process. Hence the 80/20 RDX/Al at 70% TMD produced records that can be completely resolved. These records (Fig. A7) show a process completely in accord with the physical model of DDT describing the transitional behavior of 91/9 RDX/wax at all compactations<sup>1</sup>. In other words, following a convective flame front traveling at about 0.3 mm/ $\mu$ s, a

<sup>4</sup>Belyaev, A. F., Korotkov, A. I., and Sulimov, A. A., "Breakdown of Surface Burning of Gas-Permeable Porous Systems," Combust., Explosion, and Shock Waves, Vol. 2, No. 3, 1966, 47-58.

<sup>5</sup>Korotkov, A. I., Sulimov, A. A., Obmenin, A. V., Dubovitskii, V. F., and Kurkin, A. I., "Transition from Combustion to Detonation in Porous Explosives," Combust., Explosion, and Shock Waves, Vol. 5, No. 3, 1969, 315-325.

## TABLE 1 SUMMARY OF RESULTS

Shot No.	Material	$\rho_0$ g/cm <sup>3</sup>	$\%$	Predetonation Velocities			Predet. Col. Length mm	$\Delta t_0$ μs	Relative times	D mm/μs	<u>Detonation Velocity</u>
				TMD	%	IP front mm/μs					
805	80/20 AP/Max	1.10	67.0	0.64 - 0.58	1.0	F	-	-	-	-	Class E RDX
809	"	0.93	56.6	0.73	0.6	F	-	-	-	-	Class E RDX
906	80/20 AP/Al	1.17	56.8	0.8 - 0.7	0.5	F	-	-	-	-	Class E RDX
1012	91/9 RDX/Al	1.667	89.6	2.6	-	59	7.0	-	7.56	0.34	Class E RDX
1109	"	1.324	71.2	1.7	-	58	9.0	-	6.48	0.03	Class E RDX
1118	80/20 RDX/Al	1.734	89.8	1.0	-	92 ± 10	25.0	-	~7.8	-	Class E RDX
1203	"	1.359	70.4	0.3	0.8	87	173	49	5.56	0.07	Class E RDX
810	NC	0.947	59.9	0.37 - 0.42	0.8	163	257	141	4.81	0.24	Class E RDX
905	80/20 NC/Al	0.980	57.0	0.3 - 0.7	0.7	F	-	-	-	-	Triggered on third probe
1101	NC	1.097	69.4	0.55 - 1.3	1.2	165	145	105	5.49	0.16	Class E RDX
1008	85/15 NC/AP	1.135	69.8	1.8	-	63	11.3	-	5.70	0.06	Class E RDX
1005	91/9 HMX(EE)/AP	1.324	69.5	0.98	-	86	35.5	-	6.53	0.16	Class E HMX
704 & 910	RDX(EE)	1.248	69.1	0.96	-	55-60	11-17	-	6.65	0.04	Class E RDX (See Ref. 7)
									6.88	0.06	

compression front is formed near the ignition region; it travels at 0.8 mm/ $\mu$ s (local sound speed) and marks the beginning of accelerated burning which subsequently leads to the onset of detonation. In this case, there is a rearward traveling shock which originates near the region of onset.

The effect of adding Al to RDX was to modify the transitional process; it increased  $\ell$  and  $\Delta t_D$ . This confirms the trends found with 90% TMD HMX/Al<sup>6</sup>. Earlier we found that the DDT results for pure RDX and pure HMX as well as those for waxed HMX and waxed RDX are quantitatively the same at comparable %TMD, particle size, and composition<sup>7</sup>. Here, by comparison with aluminized HMX<sup>6</sup>, we see the same equivalence in the aluminized mixtures. In addition, we find little or no difference in detonation velocity D for 9 and 20% Al at 90% TMD (also true in HMX mixes)<sup>6</sup>, no significant difference in  $\ell$  at 70 and 90% TMD, but a marked decrease in  $\Delta t_D$  as the %TMD increases from 70 to 90%.

The third group of charges consisted of NC, binary NC mixtures, and a fine HMX/AP mixture. These combinations would be expected in CMDB propellants. Records for the NC at 60 and 69% TMD (Figs. A8 and A10) are very similar to that of 80/20 RDX/Al at 70% TMD without the rearward traveling shock; they follow the same physical model. Again, increasing the %TMD did not change the  $\ell$  value but appreciably decreased the relative time to detonation  $\Delta t_D$  and decreased somewhat the time between formation of the first compression front and the onset of detonation,  $\Delta t_F$ . Addition of 20% Al to the NC resulted in a failure to transit. Hence Al hindered DDT in NC mixtures as well as in RDX mixes. On the other hand, addition of 15% AP to NC enhanced the transitional process\*, i.e., reduced both  $\ell$  and  $\Delta t_D$ . (No shot was made on 15 $\mu$  HMX, but the values should be the same as those obtained for 15 $\mu$  RDX; the latter values from Reference 7 are given for comparison in Table 1.)

The final group of charges consisted of a four-component model, a double-base gun propellant, and a plastic bonded HMX used as a gas generator. We also have for comparison, interpolated data on FKM<sup>8</sup>, a composite rocket propellant, and VLU, a CMDB rocket propellant<sup>9</sup>.

<sup>6</sup>

Price, D. and Clairmont, A. R., Jr., "Deflagration to Detonation Transition Behavior of Aluminized HMX," NSWC TR 79-119, Jun 1979.

<sup>7</sup>

Price, D. and Bernecker, R. R., "DDT Behavior of Waxed Mixtures of RDX, HMX, and Tetryl," NSWC/WOL TR 77-96, Oct 1977.

<sup>8</sup>

Bernecker, R. R. and Price, D., unpublished data.

<sup>9</sup>

Bernecker, R. R., Price, D., and Sandusky, H., "Burning to Detonation Transition in Porous Beds of High Energy Propellant," NSWC TR 79-351, Nov 1979.

\*Note the very high IP front velocity here, again indicative of the ease of onset of convective burning of AP mixtures.

The model, which was 25/5/20/50 NC/AP/A<sub>2</sub>/HMX, was at 57.3% TMD; its firing resulted in an unexpected phenomenon -- the random and erratic discharge of the first five IPs. By the time the 6th-10th pins responded in their normal sequence, the material was already detonating. In previous work, we have encountered this experimental difficulty only in coarse tetryl at high porosity<sup>10</sup>. As the porosity was decreased in the tetryl, the problem disappeared. It is highly probable that the problem would be less serious if the model were examined at lower porosities. However, the problem is quite evident at 57% TMD, and, as in the case of tetryl, must be attributed to low pressure reaction producing products of such low electrical conductivity that the IPs fail to respond to them.

Since the detonation velocity of this model was unknown, separate unconfined charges of 15.9 mm dia. were shock initiated. D, measured by probes, was

Shot	$\rho_0$ , g/cm <sup>3</sup>	%TMD	D, mm/μs
D-1009	1.096	57.1	4.84
D-1010	1.092	56.9	4.74

Since D in Shot 707 was about 4.9 mm/μs, there is no doubt that this material did achieve detonation in the transition experiment.

All possible pairs of components in this model have been examined (at least at a single ratio of contents) except NC/HMX, and these two materials have been studied separately. The only combination in which the results suggested a slight difficulty in IP response was NC/A<sub>2</sub>. Although the early IPs did not show erratic discharge, the probe record was not triggered until the third probe.

The random and erratic discharge of the early IPs suggested that different probes were discharged by different fronts instead of the customary sequential discharge by a single (the first) ionic front. SG records which recorded for only 500 μsec showed very low pressures at all locations, but one oscilloscope set to record for 700 μsec showed a rapid pressure rise at the 21 and 131 mm locations at about 580 μs (See Fig. A13b). These results suggest a longer burning time at lower pressure and a much sharper subsequent pressure rise than we have seen in most organic HE. The DDT mechanism might well be different from that of the proposed physical model.

The shredded gun propellant M-7 (67.5% TMD) showed a normal DDT record (Fig. A14) indicating that its transitional mechanism was that of the proposed physical model. Shredded Arcadene failed to transit and, at 70% TMD, produced random discharge of IPs. No records are shown here for FKM or VLU, but the latter, which contained NC and A<sub>2</sub> exhibited random and erratic discharge of the

10

Price, D., Bernecker, R. R., Erkman, J. O., and Clairmont, A. R., Jr., "DDT Behavior of Tetryl and Picric Acid," NSWC/WOL TR 76-31, May 1976.

IPs. The three 70% TMD propellants which showed DDT had a range in  $\ell$  of 103-170 mm and in  $\Delta t_D$  of 76-247  $\mu$ s.

#### SUMMARY AND CONCLUSIONS

1. 80/20 AP/fuel does not exhibit DDT at 57-67% TMD in the present setup. Fuels examined were wax and Al.
2. Addition of Al to RDX increases  $\ell$  and  $\Delta t$  at both 70 and 90% TMD. Results at 90% TMD essentially duplicate those of comparable HMX/Al compositions. Decrease of porosity from 30 to 10% did not affect  $\ell$  of RDX/Al, but did decrease  $\Delta t_D$ .
3. NC exhibited DDT at 60 and 69% TMD with the same  $\ell$  value at each porosity;  $\Delta t_D$  at 69% TMD was distinctly less than  $\Delta t_D$  at the greater porosity. Addition of Al to NC hindered transition whereas addition of AP enhanced it. Addition of AP to HMX, however, interfered with the transition.
4. The 4-component model and two different propellants exhibited random and erratic discharge of IPs at 30-43% porosity. Additional instrumentation is therefore necessary for studying some propellants at high porosity.
5. Propellants which showed a transition at 70% TMD in our apparatus, had a range of  $\ell$  of 103-170 mm and in  $\Delta t_D$  of 76-247  $\mu$ s.
6. All transitions for which complete records were obtained seemed to follow the mechanism of the original model.

BIBLIOGRAPHY

1. Bernecker, R. R. and Price, D., "Studies in the Transition from Deflagration to Detonation in Granular Explosives," Combust. Flame, Vol. 22, 1974, 111-117, 119-129, and 161-170. See also NOLTR 72-202.
2. Price, D. and Bernecker, R. R., "Sensitivity of Porous Explosives to Transition from Deflagration to Detonation," Combust. Flame, Vol. 25, 1975, 91-100. See also NOLTR 74-186.
3. Price, D., Clairmont, A. R., Jr., and Erkman, J. O., "Explosive Behavior of Aluminized Ammonium Perchlorate," Combust. Flame, Vol. 20, 1973, 389-400.
4. Belyaev, A. F., Korotkov, A. I., and Sulimov, A. A., "Breakdown of Surface Burning of Gas-Permeable Porous Systems," Combust., Explosion, and Shock Waves, Vol. 2, No. 3, 1966, 47-58.
5. Korotkov, A. I., Sulimov, A. A., Obmenin, A. V., Dubovitskii, V. F., and Kurkin, A. I., "Transition from Combustion to Detonation in Porous Explosives," Combust., Explosion, and Shock Waves, Vol. 5, No. 3, 1969, 315-325.
6. Price, D. and Clairmont, A. R., Jr., "Deflagration to Detonation Transition Behavior of Aluminized HMX," Propellants and Explosives, Vol. 4, 1979, 132-136.
7. Price, D. and Bernecker, R. R., "DDT Behavior of Waxed Mixtures of RDX, HMX, and Tetryl," NSWC/WOL TR 77-96, Oct 1977.
8. Bernecker, R. R. and Price, D., unpublished data.
9. Bernecker, R. R., Price, D., and Sandusky, H., "Burning to Detonation Transition in Porous Beds of High Energy Propellant," NSWC TR 79-351, Nov 1979.
10. Price, D., Bernecker, R. R., Erkman, J. O., and Clairmont, A. R., Jr., "DDT Behavior of Tetryl and Picric Acid," NSWC/WOL TR 76-31, May 1976.

## APPENDIX A

## DETAILED DISCUSSION OF RECORDED DATA

In previous work we have presented results from each shot as a composite illustration of distance-time and strain-time data. Here we shall follow the same scheme insofar as possible. However, in contrast to earlier work, we have examined here a large variety of 60-70% TMD charges, not a series with regular composition or compaction changes such as RDX/wax<sup>1</sup>. As a result of unpredictable variations in the DDT behavior of the present collection of charges, a number of SG records were triggered too late to give any information about predetonation conditions. Addition of aluminum to these porous charges has increased the "hash" on SG records (some hash, caused by interactions from discharge of the IPs, is always present.) When the SG record was illegible or contributed but a single point, its trace was not reproduced. The single point, which was read directly from the original polaroid record, was recorded in the table of detailed data.

The established procedure for determining the predetonation column length  $\ell$  is from the wall markings; this is then checked for consistency with the IP data in the distance-time plot. In the present results, there were three cases in which  $\ell$  could not be determined from fragment markings. In two cases, the probe data supplied an acceptable value, but in one case (that marked with an asterisk in Table A1) there was an ambiguity.

Table A1 contains the measured and assigned  $\ell$  values. Table A2 shows the rest of the detailed data for each shot.

Figs. A1-A3 show the x-t plots for three binary AP mixtures at 57-67% TMD. None exhibited transition to detonation, and all burned. The fronts outlined by the probe discharges (IP fronts) showed velocities of 0.6-0.8 mm/ $\mu$ s, high for convective fronts at this high porosity. (Fig. A1 suggests that in the case of 67% TMD 80/20 AP/wax the IP front might be caused by a pressure induced reaction. In neither of the 57% TMD charges was a similar leading pressure front detected.) Moreover, the velocity of the IP fronts in Figs. A1 and A2 appears to increase with decreasing % TMD, a trend opposite to that shown by the convective front in waxed RDX. Neither 20% Al nor 20% wax added to AP was sufficient to effect DDT in our apparatus. The IP fronts were almost identical in 80/20 AP/wax and 80/20 AP/Al, but the following compressive fronts indicated greater reaction in the ignitor region for the former.

---

<sup>1</sup>

Bernecker, R. R. and Price, D., "Studies in the Transition from Deflagration to Detonation in Granular Explosives," Combust. Flame, Vol. 22, 1974, 111-117, 119-129, and 161-170. See also NOLTR 72-202.

The next four charges are aluminized RDX at 90 and 70% TMD; all exhibited DDT. The lightly aluminized (9%) charges transited so rapidly that SG records triggered by the IP at 41 mm, showed nothing (e.g., Fig. A4) or merely a response to the detonation wave (e.g., Fig. A5). In Fig. A4 only data from the last six probes (commercial) have been used to calculate the detonation velocity. Although the WOL and commercial probes measure exactly the same detonation velocities, the former do respond slightly earlier than the latter. In this particular case, it seems preferable not to mix the two sets of data.

Addition of 9% Al to RDX at 70% has increased  $\ell$  and  $\Delta t_D$  (for RDX, the values are, respectively, 40-45 mm and 0-5  $\mu\text{s}$ <sup>7</sup>); this may also be true at 90% TMD where the values of Table A2 or Table 1 of the text can be compared to extrapolated values for HMX (45 mm and 10  $\mu\text{s}$ <sup>6</sup>), but the difference in  $\Delta t_D$  is too small to be significant. The values of  $\ell$  are, within experimental error, the same for the 70% and 90% TMD charges and so too are the values of  $\Delta t_D$ .

In Fig. A6a, the assigned  $\ell$  value of  $92 \pm 10$  mm is shown. This was a case in which  $\ell$  could not be determined from tube fragments, and its choice from the probe data was not clear-cut. For example, the response of the probe just before onset of detonation is frequently, although not always, delayed. Consequently, we used the practically identical behavior of HMX and RDX, and assigned the value obtained in 90% TMD 80/20 HMX/Al<sup>6</sup>. All values are for Class A HE, i.e.  $\delta \sim 200\mu$ , and H-5 Al. The assumed equivalence of RDX and HMX also seems justified by the close agreement of the DDT parameters:

<u>H.E.</u>	<u>9-10% Al at 90% TMD</u>	
	<u><math>\ell</math>, mm</u>	<u><math>41 \Delta t_D \mu\text{s}</math></u>
RDX	59	7.1
HMX	56	5.6
<u>20% Al at 90% TMD</u>		
RDX	(92)	25
HMX	92	23

It is evident that at 90% TMD increasing the Al content from 9 to 20% has increased  $\ell$  and  $\Delta t_D$ .

<sup>6</sup>Price, D. and Clairmont, A. R., Jr., "Deflagration to Detonation Transition Behavior of Aluminized HMX," NSWC TR 79-119, Jun 1979.

<sup>7</sup>Price, D. and Bernecker, R. R., "DDT Behavior of Waxed Mixtures of RDX, HMX, and Tetralin," NSWC/WOL TR 77-96, Oct 1977.

Fig. A7 displays the data for 70% TMD 80/20 RDX/Al. This figure shows the most complete data sets for this series of compositions. The initial IP front at 0.26 mm/ $\mu$ s is quite probably a convective wave. It is followed by a compressive wave at 0.8 mm/ $\mu$ s, a reasonable rate for 30% porous material, and that, in turn, by the onset of detonation at a rate 20% less than the ideal value for non-aluminized RDX. A shock traveling rearward from the region of onset is also evident. In other words, this transition follows exactly that proposed for waxed RDX<sup>1</sup>. It is probable that better time resolution would also demonstrate the same mechanism in the other HE/Al charges of this series.

As was the case for 91/9 RDX/Al, the initial charge compaction of the 80/20 RDX/Al had no experimentally significant effect on the value of  $\lambda$ . However, it had a very large effect on the relative time  $\Delta t_D$ ; it showed that relative time to detonation decreases as %TMD increases. The same direction of change was indicated by the 91/9 RDX/Al although 2  $\mu$ s (from 9 to 7) is not a significant difference (i.e., it is well within our experimental error).

Fig. A8 contains the data obtained on 59.9% TMD NC (Ball Powder). Fig. A8a shows that this material clearly follows the original physical model. Both the convective and postconvective fronts exhibit the appropriate velocity values for the high porosity. They also intersect about 26 mm and 25  $\mu$ s before the onset of detonation. Additional information is that the first SG ( $x=20.1$  mm) shows an excursion that might indicate a rearward traveling compression wave from  $20 < x < 67$  mm or might indicate some disturbance of the gage output near the ignitor region. The last SG ( $x=168.7$  mm) was located near the onset of detonation and responds to that event. In Fig. A8b, the record of the SG at 67 mm shows a distorted plateau, starting at about 280  $\mu$ s. If a retonation or a shock wave traveled from the onset of detonation to this SG at 4.81 mm/ $\mu$ s (the measured D), it would reach  $x=67$  at 277  $\mu$ s. Hence the plateau might have been caused by such a shock. The larger peak, which follows the plateau, begins at 303  $\mu$ s. A compression wave from  $x=\lambda=163$  mm would have to travel at 2.1 mm/ $\mu$ s to arrive at that time. However, at both 277 and 303  $\mu$ s, the strain at  $x=67$  is well above that for the yield point of the tube. Hence both details may be artifacts of the tube's plastic deformation.

Fig. A9 portrays the records from a charge of approximately the same porosity; it is NC to which 20% ~5 $\mu$  Al has been added. As Fig. A9a shows, both a convective front and a postconvective front are formed shortly after ignition. However, the pressure remains low (See Fig. A9b), and the strain does not increase rapidly to exceed the yield point until about 500  $\mu$ s (about 150  $\mu$ s after the end of the probe records). At that time, the tube probably underwent a pressure burst. Thus addition of aluminum to NC decreases its ability to undergo DDT. This was also the case for RDX above, where, however, Al delayed but did not prevent DDT. Finally, note that the first two probes did not respond to the early NC/Al reaction. Recording was triggered by the third probe.

Because most of our exploratory work was done at 70% TMD, NC was mechanically compacted to about this value. Fig. A10 displays the data which show a very similar DDT behavior to that of ~60% TMD. The details which have changed are those to be expected with a more rapid transition to detonation: front velocities are higher, intersection of the convective and postconvective fronts earlier, and the relative times ( $\Delta t_D$ ,  $\Delta t_E$ ) have decreased. On the other hand, the predetonation column length  $\ell$  has been unaffected by increasing the compaction from 60 to 70% TMD.

The previous plot for NC can be compared to that of Fig. A11 for 85/15 NC/AP. Addition of 15% ammonium perchlorate has so decreased the time required for transition that at  $x=41$  mm, the IP front is already traveling at 1.8 mm/ $\mu$ s, and the onset of detonation occurs at 63 mm. Since the SGs, triggered by the first IP, start recording late in the transitional process, only one excursion appeared and that one was a response to the detonation. Thus addition of AP to NC, decreased  $\ell$  and  $\Delta t_D$ , and had a negligible effect on D.

The effect of adding AP to a fine ( $\delta \sim 15\mu$ ) HMX was explored with a 91/9 HMX/AP mixture (see Fig. A12). It is not surprising that the reaction is again rapid and that SGs recorded little data of value. By comparison with results obtained with fine RDX<sup>7</sup>, it appears that addition of AP to HMX increases both  $\ell$  and  $\Delta t_D$ . In other words, AP decreases the tendency of HMX to undergo DDT; it has also reduced D by 8.5% below its ideal value at this %TMD.

Fig. A13 displays the data from the shot on a 57.3% TMD mixture of NC/AP/Al/HMX. In this material there was an early reaction causing random and erratic discharge of the earlier IPs. As a result the oscilloscopes for the SGs were triggered some time before the last half of the IP series which gave the D value of Fig. A13a. SGs on the oscilloscope with a sweep of about 470  $\mu$ s showed essentially no pressure change as also did those of Fig. A13b which fed into an oscilloscope set for a longer sweep. Since the pressure did not change for the first 470  $\mu$ s of recording, the plot of Fig. A13b started at ~460  $\mu$ s. The curves for the 20.8 mm and 130.7 mm locations cross, and indicate a rearward traveling shock. From the time of the pressure excursions and the separation distance, the velocity is 3.5 mm/ $\mu$ s. If this shock originates at the time and location of the onset of detonation (Fig. A13a) and travels at this constant velocity, then 541  $\mu$ s on Fig. A13b would correspond to time zero on Fig. A13a. This is the only shot included in this report for which the SG and IP records had different zero times.

There is no question that this model underwent a transition to detonation. The wall markings and the IP data clearly show this. However, the tube damage was much less than might be expected, less for instance than that for Shot 810 on NC at 59.9% TMD. A length of about 3.7 in. tube at the ignitor end was intact after the shot with the mix. It is possible that the observed DDT was of the explosive components, (e.g., HMX and NC) at high porosity, rather than the detonation of the entire mix as a composite explosive.

A modified M-7 gun propellant, 58.7/32.0/8.0/0.8/0.5 NC/NG/KP/EC/C, was shredded by cutting thin slices with a razor. The shreds were compacted to 67.5% TMD in a DDT tube in which the charge was subsequently fired. Fig. A14 shows the resultant data. As the figures show, this propellant follows the usual path for DDT. Since it was pressed to nearly 70% TMD rather than the ~60% TMD of the previous charge, it showed much more fracture damage of the containing tube.

TABLE A1  
MEASURED AND ASSIGNED  $\ell$  VALUES

Shot No.	Material	%TMD	$\ell$ Values, mm		
			From x-t Plot	From wall Markings	Assigned
805	80/20 AP/Wax	67.0			
809	"	56.6			
906	80/20 AP/Al	56.8			
1012	91/9 RDX/Al	89.6	$60\substack{+5 \\ -2}$	$59.2 \pm 2$	$59 \pm 2$
1109	"	71.2	$57\substack{+3 \\ -0}$	54.1	$58 \pm 2$
1118	80/20 RDX/Al	89.8	$75 \pm 5$	$> 59$	$92 \pm 10^*$
1203	80/20 "	70.4	$85\substack{+3 \\ -0}$	$87.1 \pm 3$	$87 \pm 3$
810	NC	59.9	$165\substack{+5 \\ -0}$	$163.3 \pm 3$	$163 \pm 3$
905	80/20 NC/Al	57.0	-	-	F
1101	NC	69.4	165	$165 \pm 3$	$165 \pm 3$
1008	85/15 NC/AP	69.8	$60\substack{+5 \\ -0}$	$63 \pm 2$	$63 \pm 2$
1005	91/9 HMX(E)/AP	69.5	$85\substack{+5 \\ -0}$	$54 < \ell < 181$	$86 \pm 2$
707	4C Model		-	$161 \pm 3$	$161 \pm 3$
816	M-7		$170 \pm 5$	-	$170 \pm 5$
1515	Arcadene		-	-	F

\*See text

TABLE A2 DETAILED DATA FOR DDT EXPERIMENTS WITH VARIOUS MATERIALS

Shot No.	805	809	906	1012
Material:	80/20 AP/Wax	80/20 AP/Wax	80/20 AP/Wax	91/9 RDX/Al
Density $\rho_0$ ( $\rho_V$ ) $\text{g/cm}^3$	1.10 (1.64)	0.93 (1.64)	1.17 (2.06)	1.667 (1.861)
%TMD	67.0	56.6	56.8	89.6
IP Data	$\frac{x}{41.4**}$	$\frac{t}{0.0**}$	$\frac{x}{41.5}$	$\frac{t}{0.0**}$
	54.1	19.7*	54.1	11.6*
	79.6	57.8*	79.5	55.1*
	104.9	89.3*	104.9	86.9*
	130.3	134.2*	130.3	130.5*
	155.8	171.5*	155.7	160.4*
	181.2	214.7*	181.2	193.7*
	206.6	261.4*	206.6	227.5*
	232.0	300.8*	232.0	261.5*
	257.3	346.6*	257.3	291.7*
SG Data	20.3	-	20.1	-
	67.7	29.5	66.4	54.5
	92.5	63.6	92.3	84.6
	118.0	87.5	117.6	136.4
	143.3	-	155.8	-
Predet. vel, $\text{mm}/\mu\text{s}$	0.64 - 0.58 1.0	0.73 0.63	22.9 0.5	0.8 - 0.7 2.6
$\lambda$ ( $\text{mm}$ )	F	F	F	F
$41\Delta t_D(\mu\text{s})$	-	-	-	59
$41\Delta t_E(\mu\text{s})$	-	-	-	7.1
$D(\sigma)$ $\text{mm}/\mu\text{s}$	-	-	-	-
				7.29(0.14)

\*Custom-made probes    \*\*NC on tip

TABLE A2 (Cont.) DETAILED DATA FOR DDT EXPERIMENTS WITH VARIOUS MATERIALS

Shot No.	1109	1118	1203	810
Material:	91/9 RDX/Al	80/20 RDX/Al	80/20 RDX/Wax	NC
Density $\rho_0(\rho_v) \text{g/cm}^3$	1.324 (1.861)	1.734 (1.934)	1.359 (1.934)	0.947 (1.58)
%TMD	71.2	89.8	70.4	59.9
IP Data	$\frac{x}{41.5}$	$\frac{t}{0.0^*}$	$\frac{x}{41.4}$	$\frac{t}{0.0^*}$
	54.12	7.50*	60.5	19.3*
	66.9	10.55*	79.5	24.0*
	79.6	12.3*	104.9	26.7*
	105.0	16.5*	130.4	30.4
	130.4	20.25*	155.8	33.9
	155.7	24.1*	181.1	36.55
	181.4	28.0*	206.5	39.4
	206.6	32.0*	225.7	41.95
	232.0	36.05*	244.7	44.35
	257.4	37.55*?	263.8	47.1
SG Data	20.6	-	20.7	-
	60.8	8.9	67.1	21.1
	79.8	-	86.1	-
	105.2	-	105.0	-
	124.2	-	130.4	-
Predet. vel., $\text{mm}/\mu\text{s}$	1.7	0.98	0.26-0.32	0.37-0.40
$x(\text{mm})$	58	92	87	163
$41\Delta t_D(\mu\text{s})$	9.0	25.0	173	257
$41\Delta t_E(\mu\text{s})$	-	-	49	141
$D(\sigma)$ $\text{mm}/\mu\text{s}$	6.48(0.03)	$\sim 7.8$	5.56(0.07)	4.81(0.24)

\*Custom-made probes

TABLE A2 (Cont.) DETAILED DATA FOR DDT EXPERIMENTS WITH VARIOUS MATERIALS

Shot No.	905	1101	1008	1005
Material:	80/20 NC/Al	NC	85/15 NC/AP	91/9 HMX(E)/AP
Density, $\rho_0 (\rho_v) g/cm^3$	0.980(1.72)	1.097(1.58)	1.135(1.63)	1.324(1.90)
%TMD	57.0	69.4	69.8	69.5
IP Data	$\frac{x}{41.5}$	$\frac{x}{41.8}$	$\frac{x}{41.5}$	$\frac{x}{41.4}$
	$\frac{t}{-*}$	$\frac{t}{0.0*}$	$\frac{t}{0.0*}$	$\frac{t}{0.0*}$
	60.6	60.8	60.6	60.6
	79.6	79.9	79.8	79.6
	0.0*	66.5*	14.44*	19.6*
	105.0	105.3	105.2	39.0*
	130.6	130.7	130.4	130.6
	156.0	149.6	143.1	155.8
	181.4	168.8	168.7	174.9
	200.3	264.9*	187.7	33.04*
	219.5	292.9*	206.9	36.55*
	238.5	319.3*	232.15	40.65*
	257.6	345.3*	257.8	257.6
			161.7*	62.0
SG Data	20.3	-	20.7	-
	66.8	83	80	20.6
	105.3	115,144	67.1	-
	136.4	182	55	-
	168.5	-	73	79.8
			97	26
			104.9	105.4
			130.3	143.1
			155.8	181.2
Predet. vel.	0.34 - 0.63	0.55 - 1.3	1.8	0.98 - 1.4
$mm/\mu s$	0.71	1.2	-	-
$\lambda (mm)$	F	165	63	86
$41\Delta t_D$	145	11.3	35.5	
$41\Delta t_E$	105	-	-	
$D(\sigma)$ $mm/\mu s$	5.49(0.16)	5.70(0.06)	6.53(0.16)	

\*Custom-made probes

TABLE A2 (Cont.) DETAILED DATA FOR DDT EXPERIMENTS WITH VARIOUS MATERIALS

Shot No.	707	816	M-7 <sup>b</sup>	84.8/15.2 HMX/HTPB <sup>c</sup>	1513
<b>Material:</b>					
Density $\rho_0 (\rho_v) \text{ g/cm}^3$	1.105(1.92)		1.10(1.63)		1.135(1.634)
%TMD	57.3		67.5		69.5
<b>IP Data</b>					
	$\frac{x}{28.70}$	$\frac{t}{-*}$	$\frac{x}{41.4}$	$\frac{t}{0.0*}$	
	54.10	-*	54.1	25.6*	
	79.50	-*	79.6	70.45*	
	104.90	-*	105.0	90.35*	
	130.30	-*	130.3	111.05*	
	155.70	0	155.7	119.10*	
	181.23	5.08*	181.2	125.45*	
	206.63	10.93	206.6	131.10*	
	232.03	15.86	231.9	136.55*	
	257.43	20.82	257.3	140.85*	
<b>SG Data</b>					
	20.8	510,581 <sup>d</sup>	20.8	-	
	54.4	-	67.1	53	
	80.3	-	105.4	79	
	104.9	-	136.9	105	
	130.7	550	168.8	-	
<b>Predeton. vel.</b>					
	-		0.50 - 1.28	-	
	$\frac{mm}{\mu s}$		1.34		
	$\frac{g}{mm}$				
	$41\Delta t_D(\mu s)$	161	170		
	$41\Delta t_E(\mu s)$	-	124		
	$D(\sigma), \text{ mm}/\mu s$	~4.9	91		
				4.89(0.21)	

A-10

a. 25/5/20/50 NC/AP/AP/HMX b. Double base powder: 58.7/32.0/8.0/0.8/0.5 NC/NG/KC104/EC/C shredded;  
 c. Shredded; d. Oscilloscopes triggered during random and erratic discharge of IPs prior to series recorded above; time scales differ.

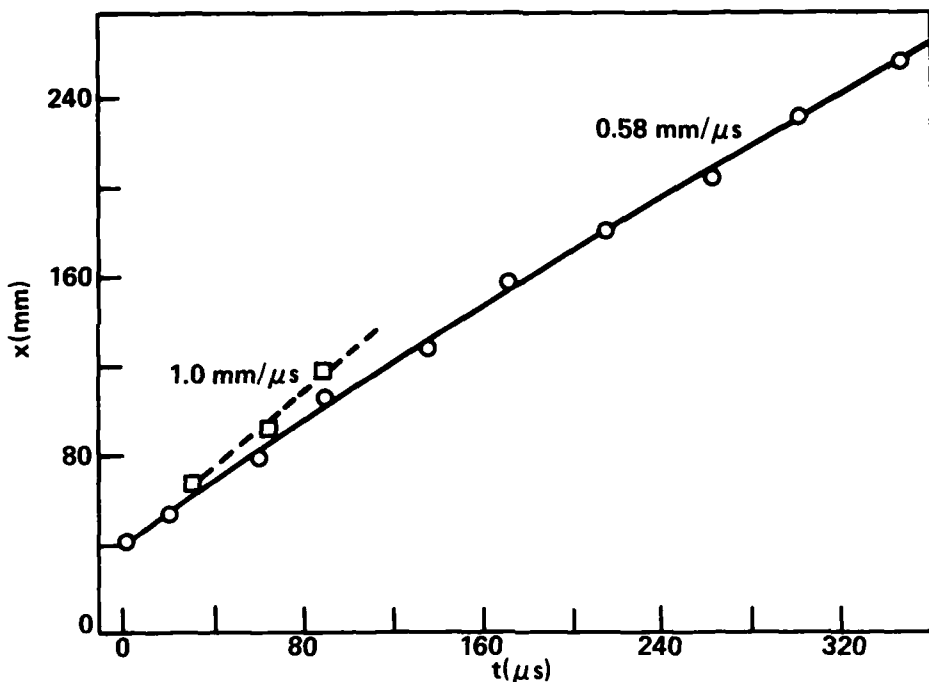


FIGURE A1 DISTANCE-TIME DATA FROM SHOT 805 ON 80/20 AP/WAX AT 67.0% TMD,  $\rho_0 = 1.10$  g/cm<sup>3</sup>. (○ WOL PROBE, ● COMMERCIAL PROBE, □ PRESSURE EXCURSION)

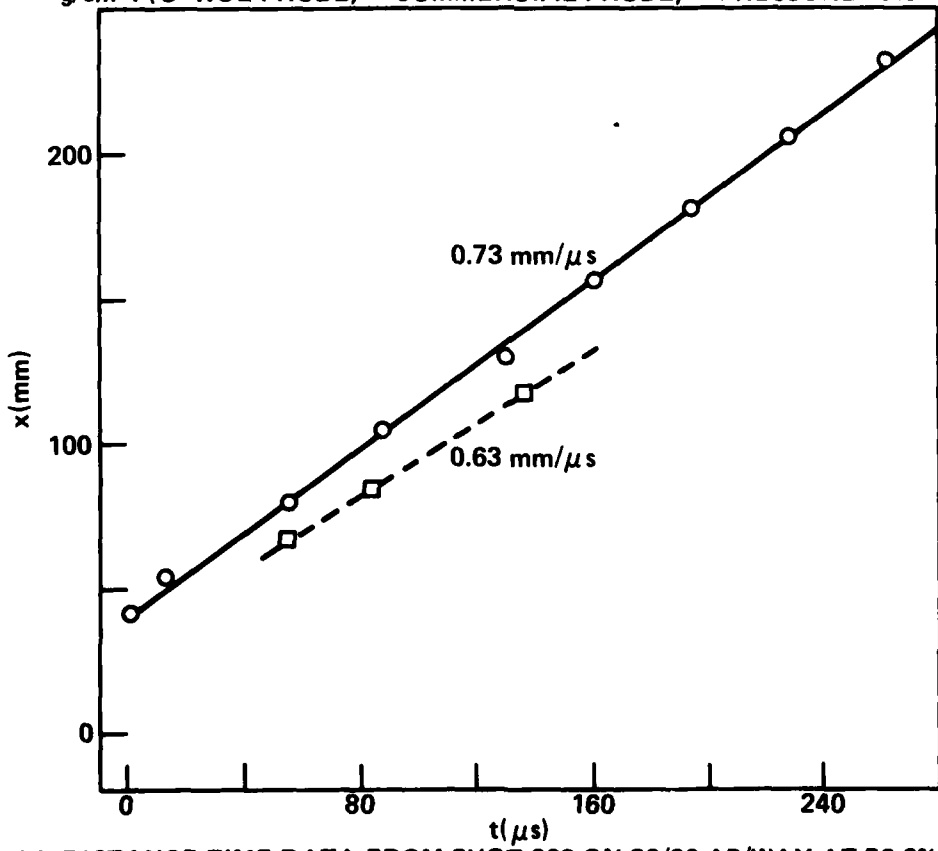
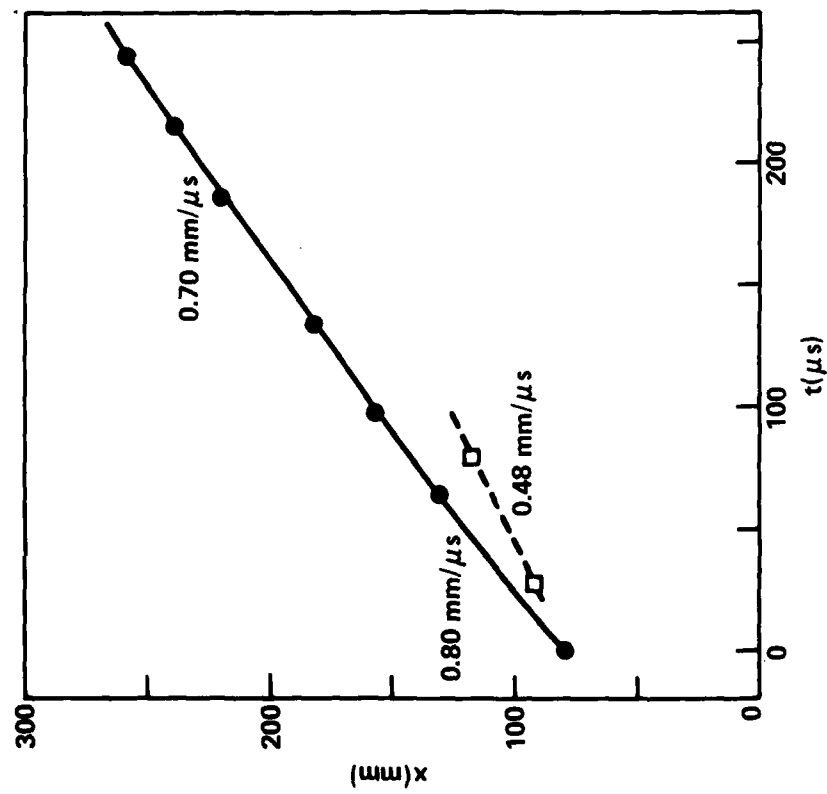
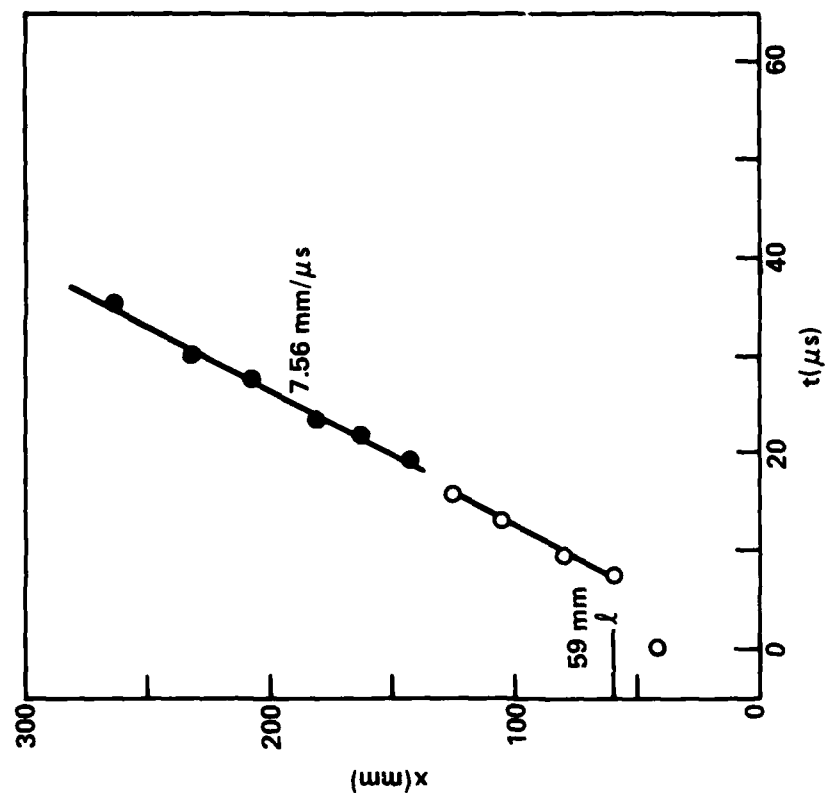


FIGURE A2 DISTANCE-TIME DATA FROM SHOT 809 ON 80/20 AP/WAX AT 56.6% TMD,  $\rho_0 = 0.93$  g/cm<sup>3</sup>. (KEY OF FIGURE A1)



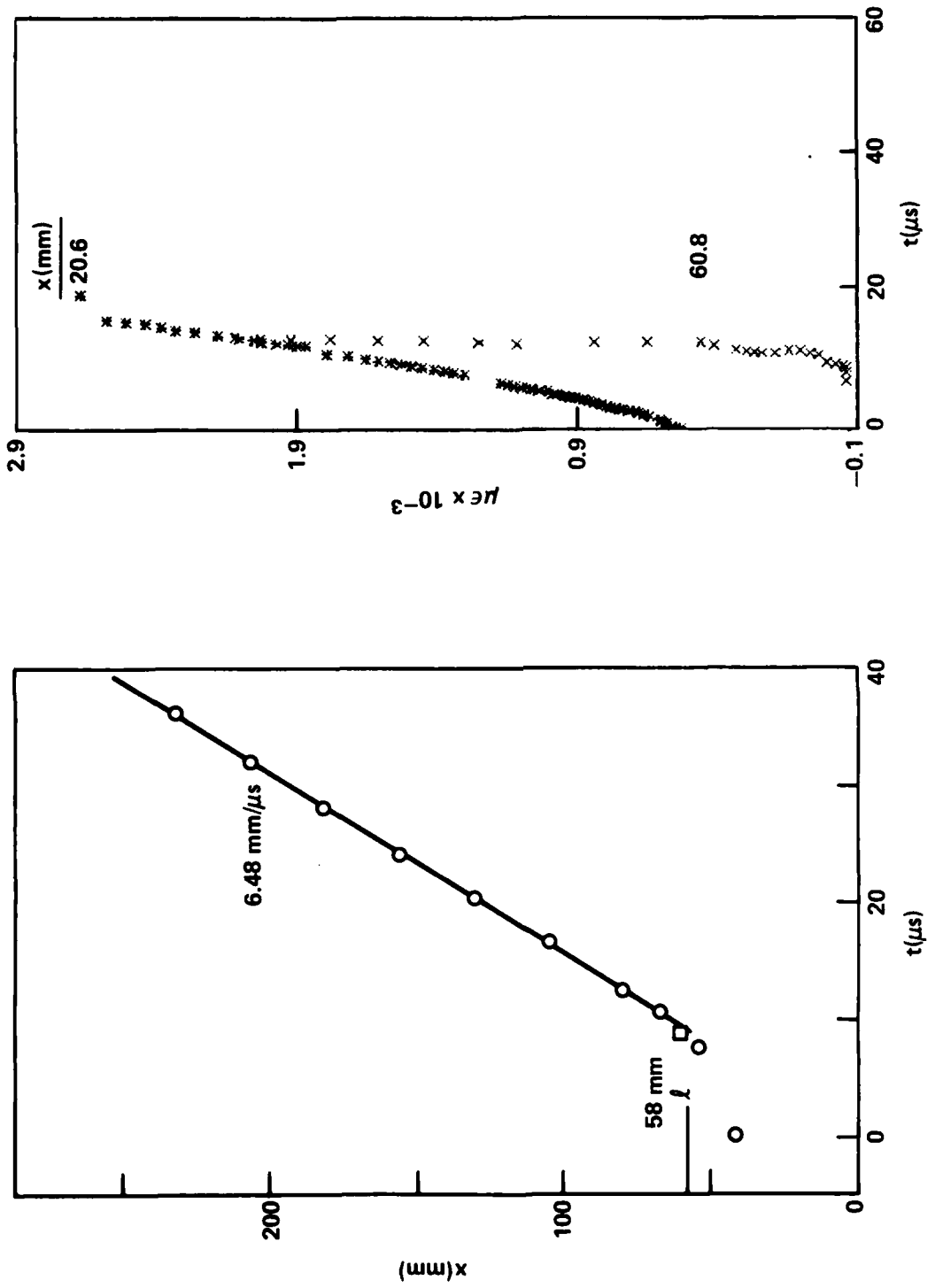


FIGURE A5 DATA FROM SHOT 1109 ON 91/9 RDX/Al AT 71.2% TMD,  $\rho_0 = 1.32 \text{ g/cm}^3$

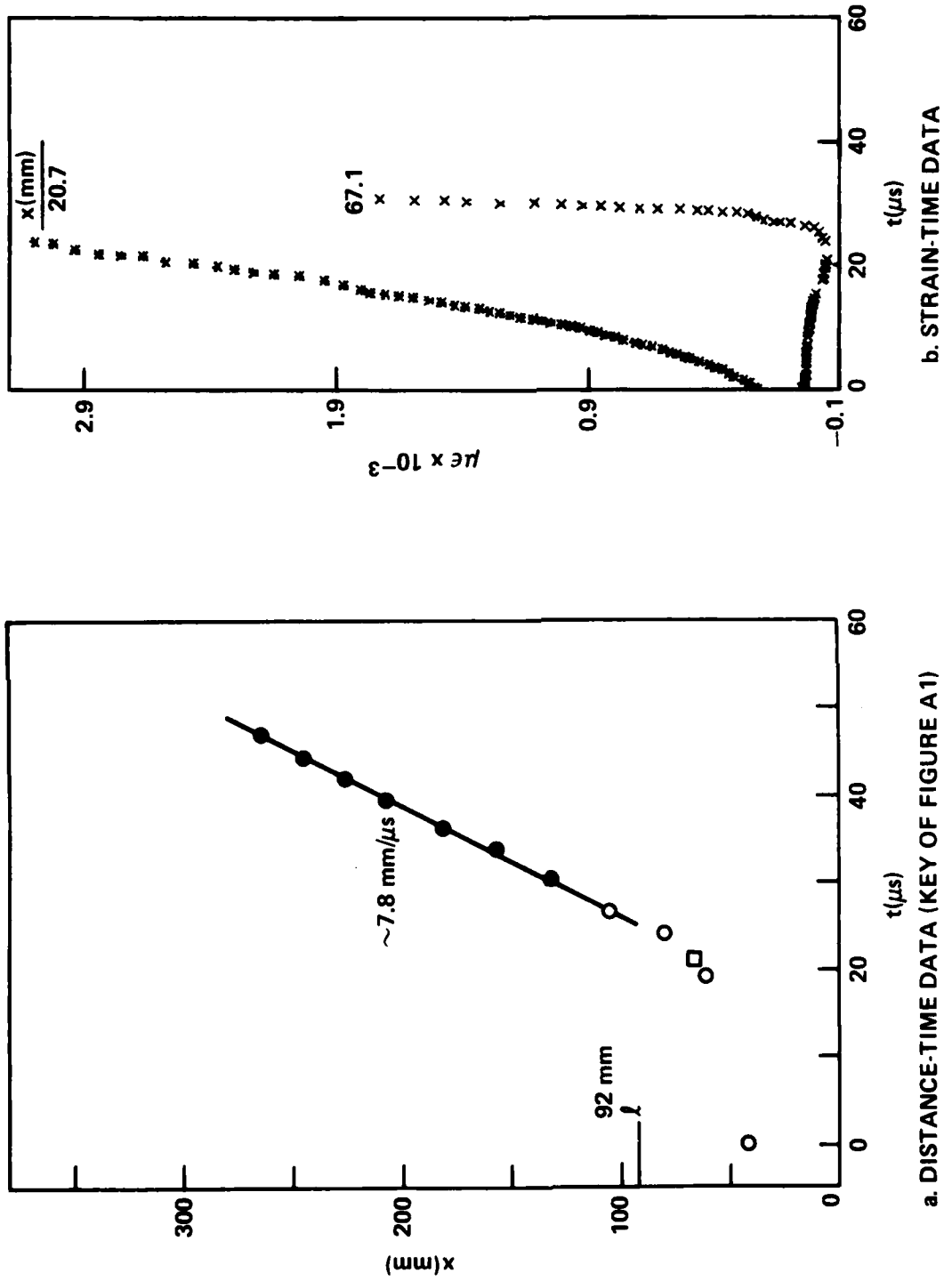
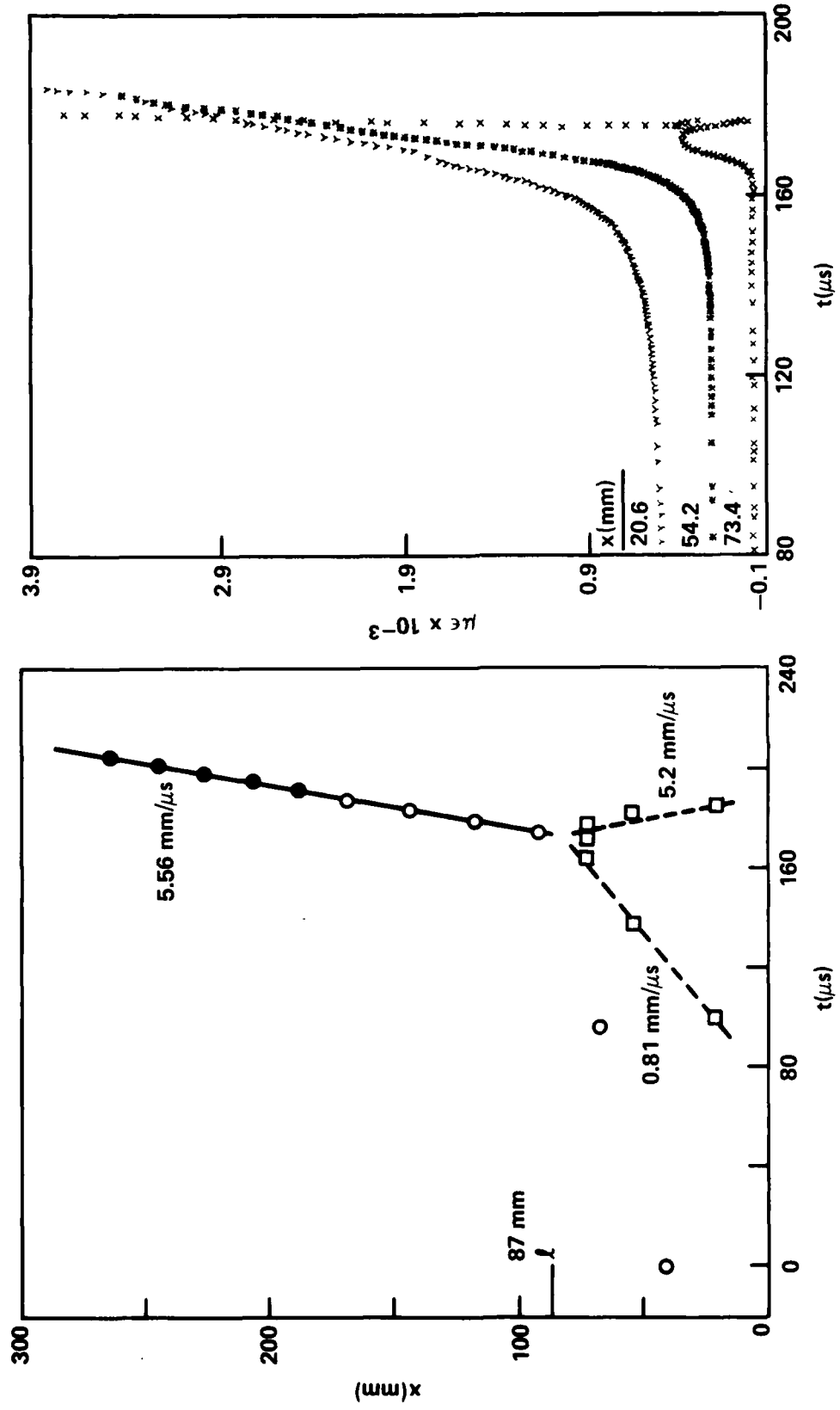


FIGURE A6 DATA FROM SHOT 1118 ON 80/20 RDX/Al AT 89.8% TMD,  $\rho_0 = 1.73 \text{ g/cm}^3$



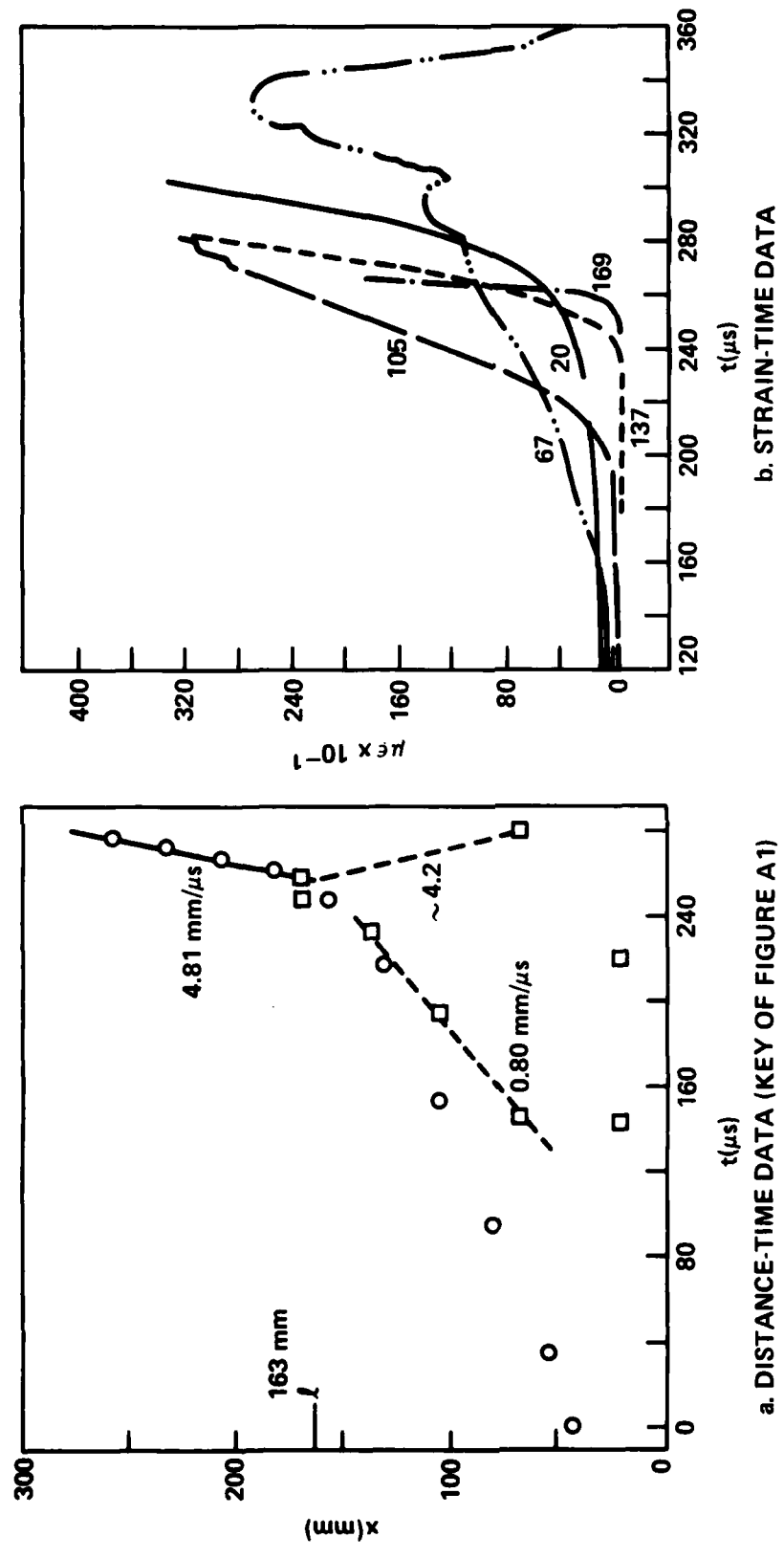
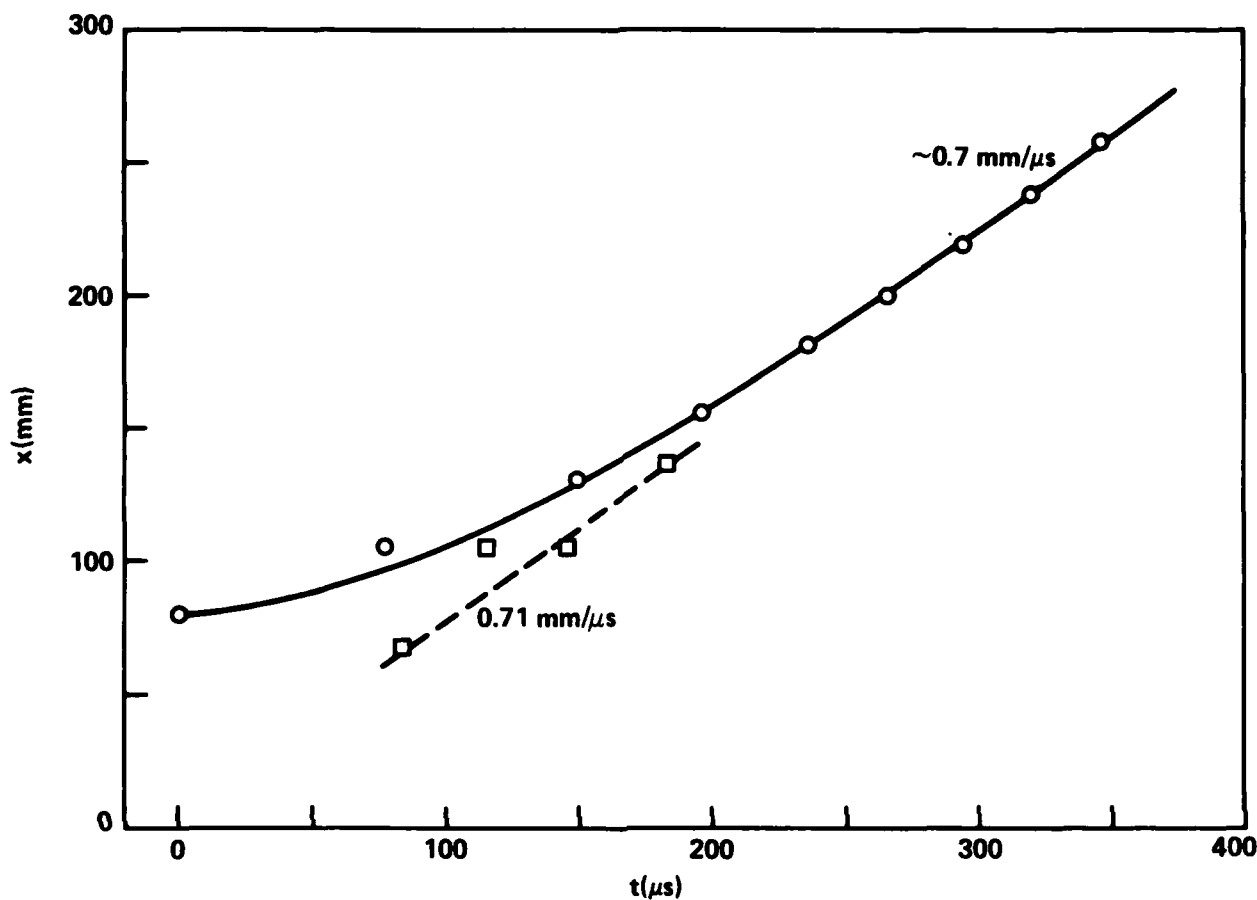


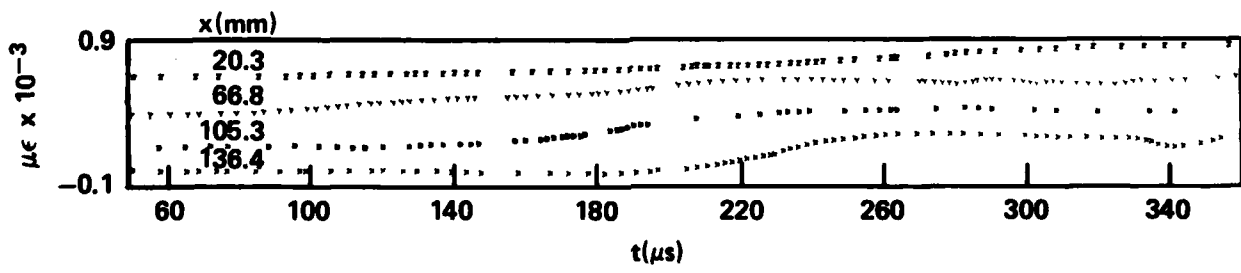
FIGURE A8 DATA FROM SHOT 810 ON NC AT 59.9% TMD,  $\rho_0 = 0.95 \text{ g/cm}^3$

b. STRAIN-TIME DATA

a. DISTANCE-TIME DATA (KEY OF FIGURE A1)

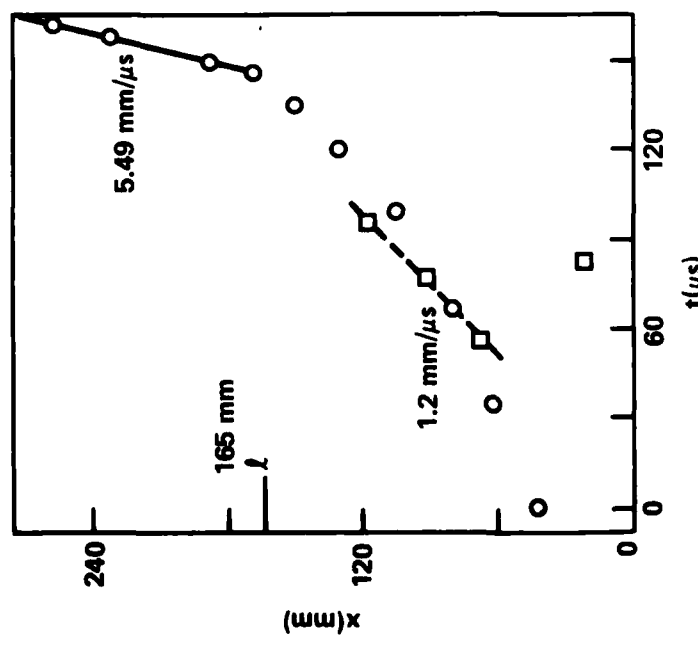
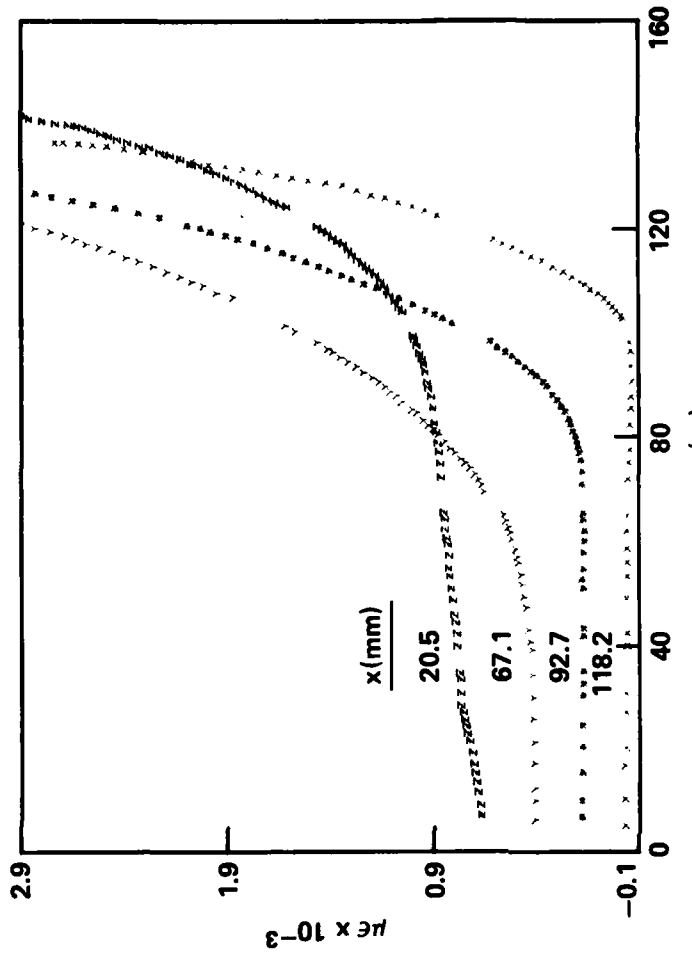


a. DISTANCE-TIME DATA (KEY OF FIGURE A1)



b. STRAIN-TIME DATA (KEY OF FIGURE A7b)

FIGURE A9 DATA FROM SHOT 905 ON 80/20 NC/Al AT 57.0% TMD,  $\rho_0 = 0.98 \text{ g}/\text{cm}^3$



A-18

a. DISTANCE-TIME DATA (KEY OF FIGURE A1)

b. STRAIN-TIME DATA (KEY OF FIGURE A7b)

FIGURE A10 DATA FROM SHOT 1101 ON NC AT 69.4% TMD,  $\rho_o = 1.10 \text{ g/cm}^3$

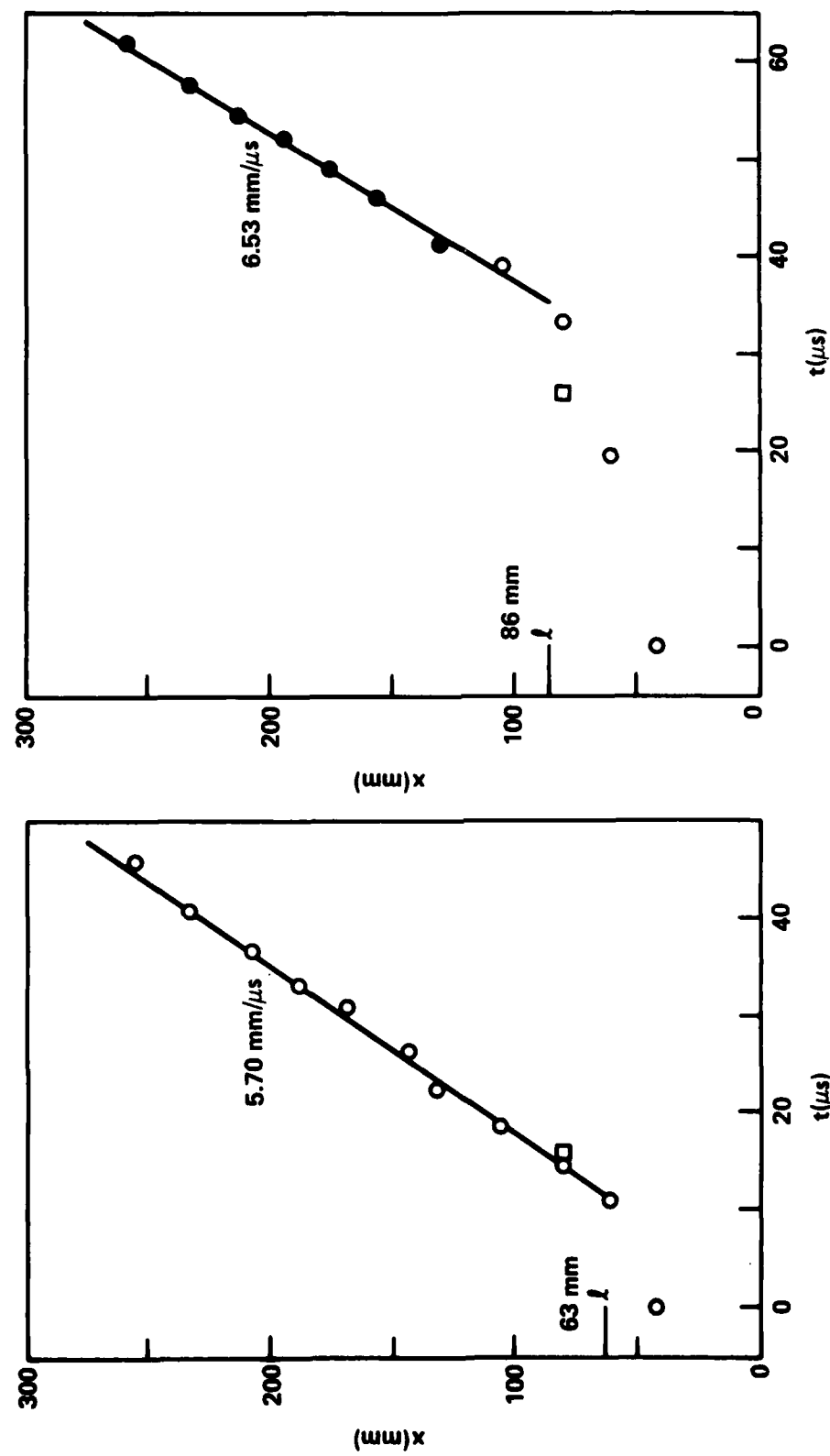


FIGURE A12 DISTANCE-TIME DATA FROM SHOT 1005 ON 919 HMX/AP AT 69.5% TMD,  $\rho_0 = 1.32 \text{ g/cm}^3$ .  
(KEY OF FIGURE A1)

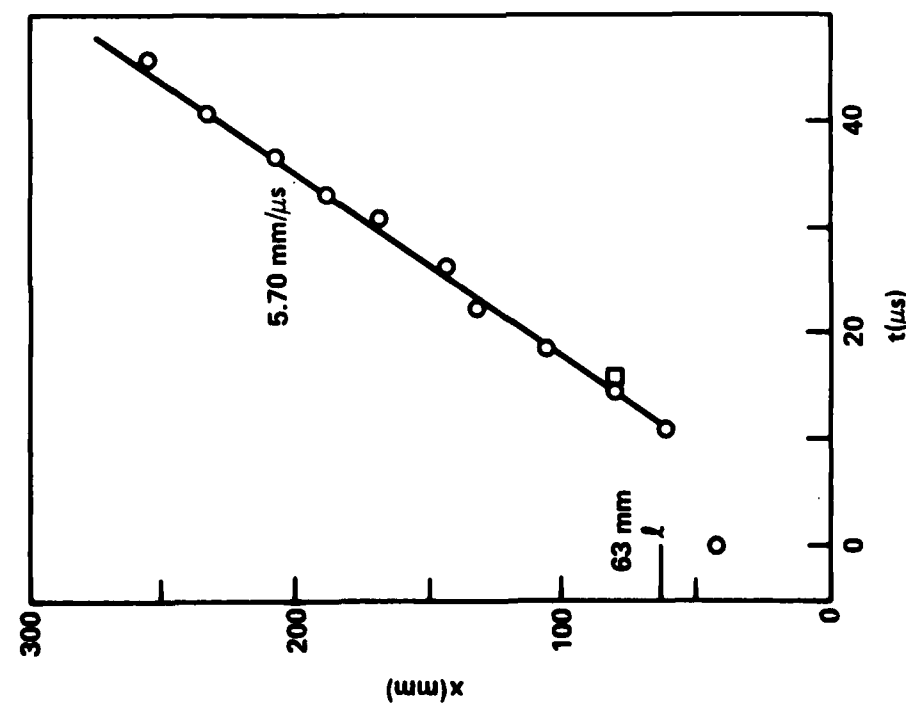


FIGURE A11 DISTANCE-TIME DATA FROM SHOT 1008 ON 85/15 NC/AP AT 69.8% TMD,  
 $\rho_0 = 1.14 \text{ g/cm}^3$ . (KEY OF FIGURE A1)

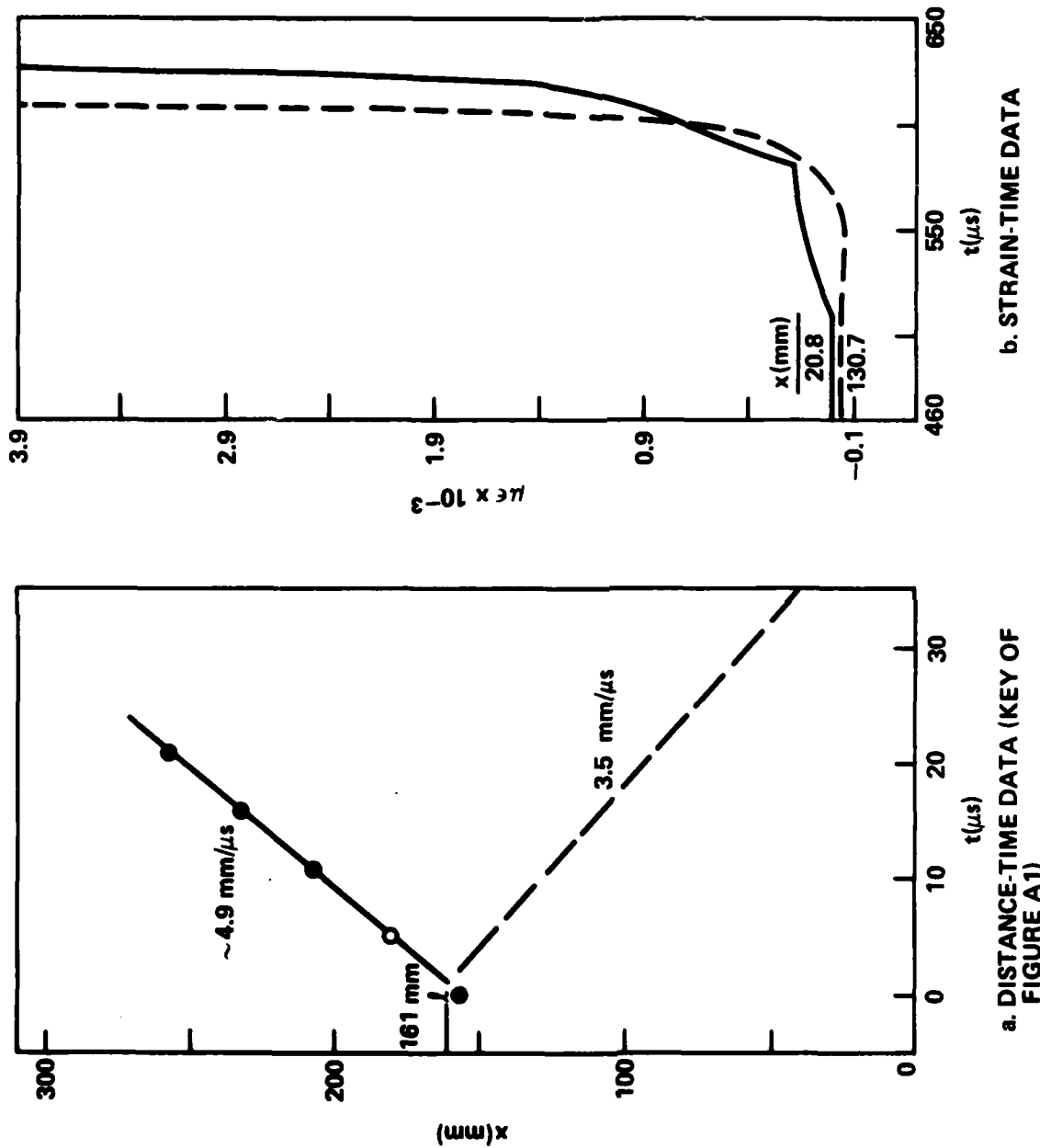
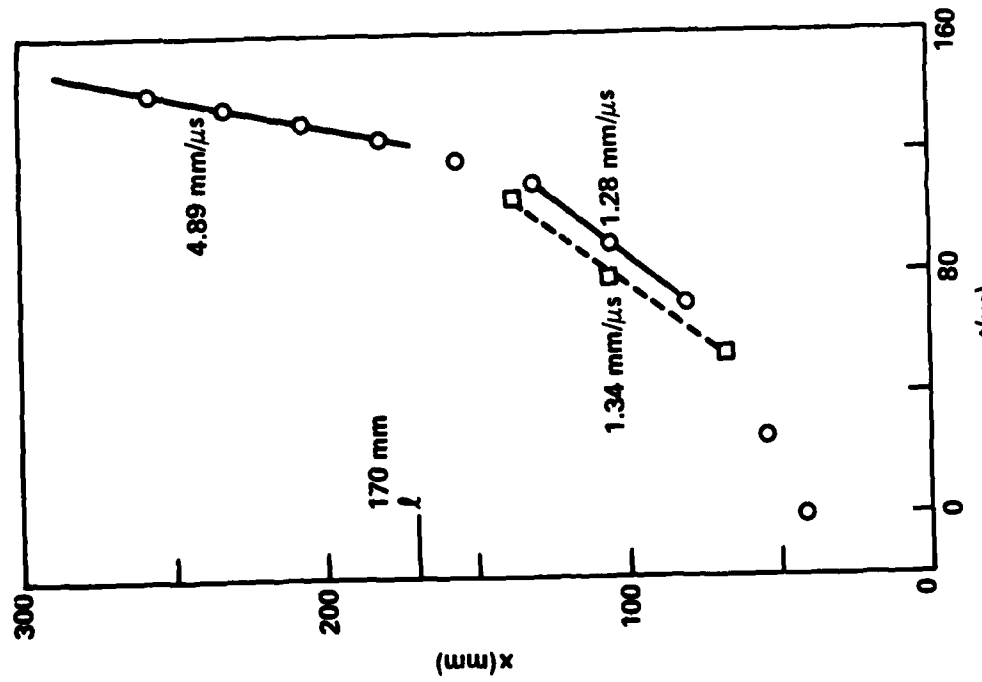
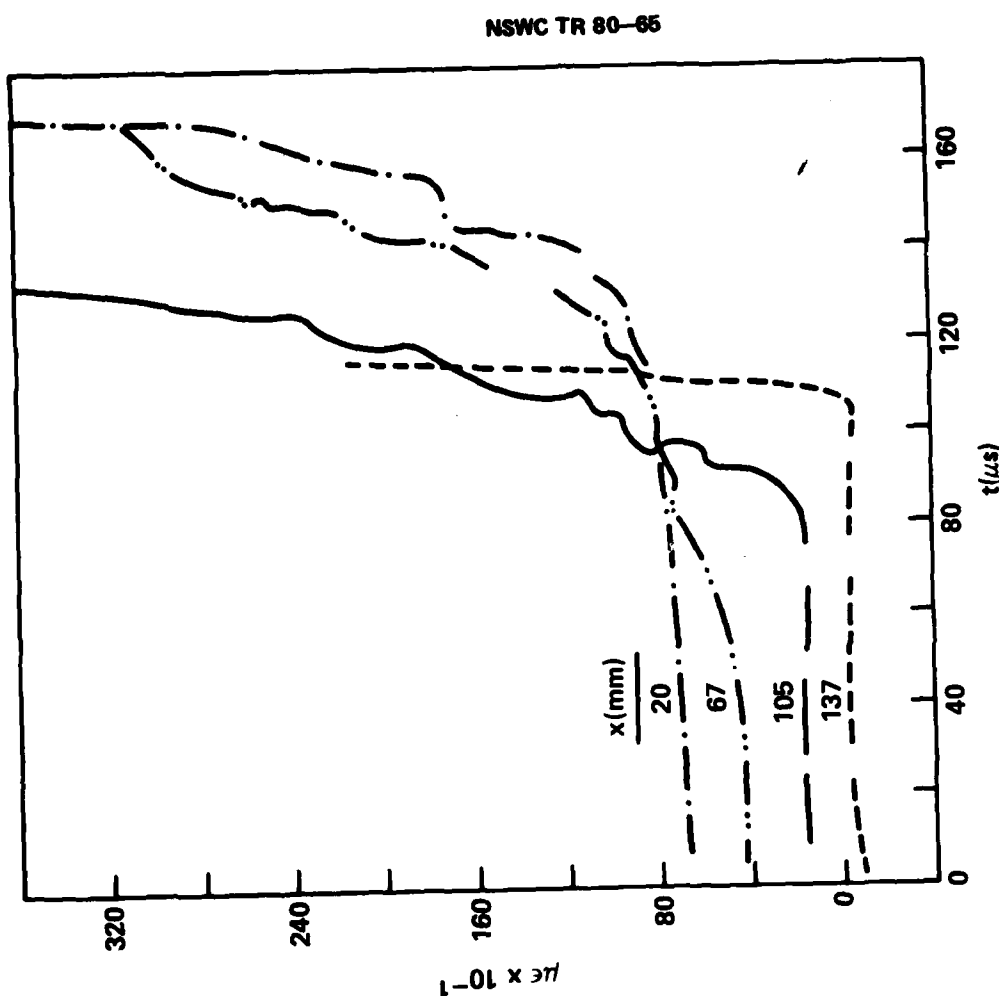


FIGURE A13 DATA FROM SHOT 707 ON 57.3% TMD 25/5/20/50 NC/AP/Al /HMX,  $\rho_0 = 1.11 \text{ g/cm}^3$



A-21

FIGURE A14 DATA FROM SHOT 816 ON 67.5% TMD DOUBLE BASE POWDER M-7,  $\rho_0 = 1.10 \text{ g/cm}^3$

b. STRAIN-TIME DATA (KEY OF FIGURE A7b)

a. DISTANCE-TIME DATA (KEY OF FIGURE A1)

**DISTRIBUTION**

**Chief of Naval Material**  
**Washington, DC 20360**

**Commander**  
**Naval Air Systems Command**  
**Attn: AIR-350**  
**AIR-330**  
**Department of the Navy**  
**Washington, DC 20361**

**Commander**  
**Naval Sea Systems Command**  
**Attn: Technical Library**  
**SEA-03B**  
**SEA-62R**  
**SEA-62R2**  
**SEA-62R3**  
**SEA-62R32**  
**SEA-64E**  
**Department of the Navy**  
**Washington, DC 20362**

2

**Director**  
**Strategic Systems Project Office (PM-1)**  
**Attn: SP-273 (R. M. Kinert)**  
**SP-27311 (E. L. Throckmorton, Jr.)**  
**Department of the Navy**  
**Washington, DC 20376**

**Office of Naval Research**  
**Attn: Rear Admiral A. J. Baciocco, Jr.**  
**ONR-741 (Technical Library)**  
**ONR-473 (R. S. Miller)**  
**Department of the Navy**  
**800 North Quincy Street**  
**Arlington, VA 22217**

DISTRIBUTION (Cont.)

Commander  
Naval Weapons Center  
Attn: Code 556  
Technical Library  
H. D. Mallory  
Code 452  
Code 5008  
Code 3264  
Code 3205 (C. Thelin)  
Code 32052 (L. Smith)  
R. L. Derr  
China Lake, CA 93555

Director  
Naval Research Laboratory  
Attn: Technical Information Section  
Washington, DC 20375

2

Office of Chief of Naval Operations  
Operations Evaluation Group (OP03EG)  
Washington, DC 20350

Director  
Office of the Secretary of Defense  
Advanced Research Projects Agency  
Washington, DC 20301

Commanding Officer  
Naval Weapons Station  
Attn: R&D Division  
Code 50  
Yorktown, VA 23691

Commanding Officer  
Naval Propellant Plant  
Attn: Technical Library  
Indian Head, MD 20640

Commanding Officer  
Naval Explosive Ordnance Disposal Facility  
Attn: Information Services  
Indian Head, MD 20640

McDonnell Aircraft Company  
Attn: M. L. Schimmel  
P. O. Box 516  
St. Louis, MO 63166

DISTRIBUTION (Cont.)

Commanding Officer  
Naval Ammunition Depot  
Crane, IN 47522

Commanding Officer  
Naval Underwater Systems Center  
Attn: LA 151-Technical Library  
Newport, RI 02840

Commanding Officer  
Naval Weapons Evaluation Facility  
Attn: Code AT-7  
Kirtland Air Force Base  
Albuquerque, NM 87117

Commanding Officer  
Naval Ammunition Depot  
Attn: QEL  
Concord, CA 94522

Superintendent Naval Academy  
Attn: Library  
Annapolis, MD 21402

Naval Plant Representative Office  
Strategic Systems Project Office  
Lockheed Missiles and Space Company  
Attn: SPL-332 (R. H. Guay)  
P. O. Box 504  
Sunnyvale, CA 94088

Hercules Incorporated  
Allegany Ballistics Laboratory  
Attn: Library  
P. O. Box 210  
Cumberland, MD 21502

AMCRD  
5001 Eisenhower Avenue  
Alexandria, VA 22302

Redstone Scientific Information Center  
U. S. Army Missile Command  
Attn: Chief, Documents  
Redstone Arsenal, AL 35809

2

DISTRIBUTION (Cont.)

Commanding Officer  
Army Armament Research and  
Development Command  
Energetic Materials Division  
Attn: Louis Avrami, DRDAR-LCE  
Dover, NJ 07801

Commanding General  
Attn: BRL Library  
DRDAR-BLT (P. Howe)  
Aberdeen Proving Ground, MD 21005

Commanding Officer  
Harry Diamond Laboratories  
Attn: Library  
2800 Powder Mill Road  
Adelphi, MD 20783

Armament Development & Test Center  
DLOSL/Technical Library  
 Eglin Air Force Base, Florida 32542

Commanding Officer  
Naval Ordnance Station  
Louisville, KY 40124

Director  
Applied Physics Laboratory  
Attn: Library  
Johns Hopkins Road  
Laurel, MD 20810

U. S. Department of Energy  
Attn: DMA  
Washington, DC 20545

Director  
Defense Nuclear Agency  
Washington, DC 20305

Research Director  
Pittsburgh Mining and Safety  
Research Center  
Bureau of Mines  
4800 Forbes Avenue  
Pittsburgh, PA 15213

2

DISTRIBUTION (Cont.)

Director  
Defense Technical Information Center  
Cameron Station  
Alexandria, VA 22314

12

Goddard Space Flight Center, NASA  
Glenn Dale Road  
Greenbelt, MD 20771

Lawrence Livermore Laboratory  
University of California  
Attn: M. Finger  
E. James  
E. Lee  
P. Urtiew  
C. Tarver  
P. O. Box 808  
Livermore, CA 94551

Sandia Laboratories  
Attn: R. J. Lawrence, Div. 5166  
P. O. Box 5800  
Albuquerque, NM 87115

Director  
Los Alamos Scientific Laboratory  
Attn: Library  
L. C. Smith  
B. G. Craig  
H. Flaugh  
P. O. Box 1663  
Los Alamos, NM 87544

Chairman  
DOD Explosives Safety Board  
Attn: Dr. T. A. Zoker  
2461 Eisenhower Avenue  
Alexandria, VA 22331

Aerojet Ordnance and Manufacturing  
Company  
9236 East Hall Road  
Downey, CA 90241

Hercules Incorporated Research Center  
Attn: Technical Information Division  
B. E. Clouser  
Wilmington, DE 19899

DISTRIBUTION (Cont.)

Thiokol/Huntsville Division  
Attn: Technical Library  
Huntsville, AL 35807

Shock Hydrodynamics Division  
Whittaker Corporation  
Attn: Dr. L. Zernow  
4716 Vineland Avenue  
North Hollywood, CA 91706

Stanford Research Institute  
Attn: D. Curran  
333 Ravenswood Avenue  
Menlo Park, CA 94025

Thiokol/Wasatch Division  
Attn: Technical Library  
P. O. Box 524  
Brigham City, UT 84302

Thiokol/Elkton Division  
Attn: Technical Library  
P. O. Box 241  
Elkton, MD 21921

Teledyne McCormick Selph  
P. O. Box 6  
Hollister, CA 95023

Lockheed Missiles and Space Co., Inc.  
P. O. Box 504  
Sunnyvale, CA 94086

R. Stresau Laboratory, Inc.  
Star Route  
Spooner, WI 54801

Rohm and Haas  
Huntsville, Defense Contract Office  
Attn: H. M. Shuey  
723-A Arcadia Circle  
Huntsville, AL 35801

2

DISTRIBUTION (Cont.)

U. S. Army Foreign Service  
and Technology Center  
220 7th Street, N.E.  
Charlottesville, VA 22901

Princeton Combustion Research Laboratories, Inc.  
1041 U. S. Highway One North  
Attn: M. Summerfield  
N. Messina  
Princeton, NJ 08540

Pennsylvania State University  
Department of Mechanical Engineering  
Attn: K. Kuo  
University Park, PA 16802

Ballistic Research Laboratories  
Attn: N. Gerri  
Aberdeen Proving Ground, MD 21005

Paul Gough Associates  
1048 South Street  
Portsmouth, NH 03801

Hercules Incorporated, Bacchus Works  
Attn: B. Hopkins  
Library 100-H  
P. O. Box 98  
Magna, UT 84044

Professor H. Krier  
A & A Engineering Department  
101 Transportation Building  
University of Illinois  
Urbana, IL 61801

Chemical Propulsion Information Agency  
The Johns Hopkins University  
Applied Physics Laboratory  
Johns Hopkins Road  
Laurel, MD 20810

ITT Research Institute  
Attn: H. S. Napadensky  
10 West 35th Street  
Chicago, IL 60616

DISTRIBUTION (Cont.)

Erion Associates, Inc.  
Attn: W. Petray  
600 New Hampshire Avenue,  
Suite 870  
Washington, DC 20037

Brigham Young University  
Department of Chemical Engineering  
Attn: Dr. M. W. Beckstead  
Provo, UT 84601  
Library of Congress  
Washington, D. C. 20540  
Attn: Gift And Exchange Division

4

TO AID IN UPDATING THE DISTRIBUTION LIST  
FOR NAVAL SURFACE WEAPONS CENTER, WHITE  
OAK TECHNICAL REPORTS PLEASE COMPLETE THE  
FORM BELOW:

TO ALL HOLDERS OF NSWC/TR 80-65  
by Donna Price, Code R10

DO NOT RETURN THIS FORM IF ALL INFORMATION IS CURRENT

A. FACILITY NAME AND ADDRESS (OLD) (Show Zip Code)

NEW ADDRESS (Show Zip Code)

B. ATTENTION LINE ADDRESSES:

C.

REMOVE THIS FACILITY FROM THE DISTRIBUTION LIST FOR TECHNICAL REPORTS ON THIS SUBJECT.

D.

NUMBER OF COPIES DESIRED

DEPARTMENT OF THE NAVY  
NAVAL SURFACE WEAPONS CENTER  
WHITE OAK, SILVER SPRING, MD. 20910

OFFICIAL BUSINESS  
PENALTY FOR PRIVATE USE, \$300

POSTAGE AND FEES PAID  
DEPARTMENT OF THE NAVY  
DOD 316



COMMANDER  
NAVAL SURFACE WEAPONS CENTER  
WHITE OAK, SILVER SPRING, MARYLAND 20910

ATTENTION COMM 220